Meteoritics & Planetary Science 39, Nr 1, 31–51 (2004)
Abstract available online at http://meteoritics.org

Geochemistry and shock petrography of the Crow Creek Member, South Dakota, USA: Ejecta from the 74-Ma Manson impact structure

Crispin KATONGO,[1] Christian KOEBERL,[1]* Brian J. WITZKE,[2] Richard H. HAMMOND,[3] and Raymond R. ANDERSON[2]

[1]Department of Geological Sciences, University of Vienna, Althanstrasse 14, A-1090, Vienna, Austria
[2]Iowa Geological Survey, Iowa City, Iowa 52242–1319, USA
[3]Hammond-Wetmore Drilling Company, Vermillion, South Dakota 57069, USA
*Corresponding author. E-mail: christian.koeberl@univie.ac.at

(Received 11 July 2003; revision accepted 9 December 2003)

Abstract–The Crow Creek Member is one of several marl units recognized within the Upper Cretaceous Pierre Shale Formation of eastern South Dakota and northeastern Nebraska, but it is the only unit that contains shock-metamorphosed minerals. The shocked minerals represent impact ejecta from the 74-Ma Manson impact structure (MIS). This study was aimed at determining the bulk chemical compositions and analysis of planar deformation features (PDFs) of shocked quartz; for the basal and marly units of the Crow Creek Member. We studied samples from the Gregory 84-21 core, Iroquois core and Wakonda lime quarry. Contents of siderophile elements are generally high, but due to uncertainties in the determination of Ir and uncertainties in compositional sources for Cr, Co, and Ni, we could not confirm an extraterrestrial component in the Crow Creek Member. We recovered several shocked quartz grains from basal-unit samples, mainly from the Gregory 84-21 core, and results of PDF measurements indicate shock pressures of at least 15 GPa. All the samples are composed chiefly of SiO_2 (29–58 wt%), Al_2O_3 (6–14 wt%), and CaO (7–30 wt%). When compared to the composition of North American Shale Composite, the samples are significantly enriched in CaO, P_2O_5, Mn, Sr, Y, U, Cr, and Ni. The contents of rare earth elements (REE), high field strength elements (HFSE), Cr, Co, Sc, and their ratios and chemical weathering trends, reflect both felsic and basic sources for the Crow Creek Member, an inference, which is consistent with the lithological compositions in the environs of the MIS. The high chemical indices of alteration and weathering (CIA' and CIW': 75–99), coupled with the Al_2O_3-(CaO*+Na_2O)-K_2O (A-CN'-K) ratios, indicate that the Crow Creek Member and source rocks had undergone high degrees of chemical weathering. The expected ejecta thicknesses at the sampled locations (409 to 219 km from Manson) were calculated to range from about 1.9 to 12.2 cm (for the present-day crater radius of Manson), or 0.4 to 2.4 cm (for the estimated transient cavity radius). The trend agrees with the observed thicknesses of the basal unit of the Crow Creek Member, but the actually observed thicknesses are larger than the calculated ones, indicating that not all of the basal unit comprises impact ejecta.

INTRODUCTION

Distal ejecta are those ejecta that occur at considerable distances (commonly defined as >5 crater radii from the crater rim) from the source crater (Melosh 1989; French 1998). They either consist of fine-grained rock and mineral fragments or glasses (Montanari and Koeberl 2000). Distal ejecta are important as markers for impact events in the stratigraphic record. The most commonly used impact indicators in ejecta layers are elevated contents of siderophile elements, especially Ir and other platinum group elements (PGE), spherules and/or the presence of shocked minerals, particularly quartz (e.g., Alvarez et al. 1980; Bohor et al. 1984; Koeberl and Sigurdsson 1992; Izett et al. 1993). Correlation of ejecta layers in the stratigraphic record with source impact structures allows a comparison to be made between impact structure sizes, target lithologies and ejecta distribution with changes in biota across the layer (e.g., Montanari and Koeberl 2000; Koeberl 2001).

The discovery of impact-shocked mineral grains in the Crow Creek Member of the Upper Cretaceous Pierre Shale Formation (Izett et al. 1993), which has a biostratigraphic age

of about 74 Ma, led to the interpretation that shocked minerals represent distal impact ejecta (Koeberl and Anderson 1996; Witzke et al. 1996; Izett et al. 1998) of the coeval Manson impact structure (MIS), a 37-km diameter impact structure in Iowa. The MIS has a radiometric age of 74.1 Ma (Izett et al. 1998). The Crow Creek Member is one of the several marly units recognized within the Upper Cretaceous Pierre Shale of eastern South Dakota and northeastern Nebraska, and forms a prominent light-colored band in the otherwise dark Lower Pierre Shale outcrops (Witzke et al. 1996). However, it is unique in that it is the only unit in the Pierre Shale containing shock-metamorphosed mineral grains. Although making up only a small percentage of the Pierre Shale, it is widely distributed and extends from near Yankton (South Dakota) for 300 km northeast to Pierre (South Dakota) mainly along the Missouri river (Izett et al. 1998) (Fig.1).

The mode of deposition of the Crow Creek Member still remains a matter of discussion. Some researchers suggest an impact-triggered tsunami deposit (Steiner and Shoemaker 1996; Izett et al. 1998), while others favor normal transgressive sedimentation (Witzke et al. 1996). However, there is general consensus that the shocked minerals in the Crow Creek Member were derived from the MIS and that the unit is composed of both allochthonous and autochthonous inputs.

Most of the (few) studies on the Crow Creek Member have focused on depositional processes, stratigraphy, paleontology, and petrography. Apart from mineral analyses of shocked feldspars by Koeberl et al. (1996), no other compositional data are available. In this paper, we present results of shock petrography and bulk chemical compositions of the basal and marly units of the Crow Creek Member of samples from Gregory 84-21 core (GC), Iroquois core (IC), and Wakonda lime quarry (WLQ) located at 409, 300 and 219 km from the center of the MIS, respectively (Fig. 1). In an effort to ascertain the presence of an extraterrestrial component, we also determined the Cr, Co, Ni, and Ir contents. We performed universal stage measurements on a few shocked-quartz grains that were recovered from some basal-unit samples. On the basis of bulk chemistry, we have evaluated provenance and weathering characteristics of the Crow Creek Member.

GEOLOGICAL AND PETROGRAPHIC FRAMEWORK

Detailed geological and petrographic descriptions of the Crow Creek Member are presented by, e.g., Bretz (1979), Izett et al. (1993) and Witzke et al. (1996). Because the present study was mainly focused on bulk chemical compositions of the Crow Creek Member and measurement of PDFs in shocked quartz, we present here a summary of previous work, mainly drawn from the above references, in order to provide geological and petrographic context for the discussion of our results.

The Crow Creek Member is a marl-dominated interval within the Upper Cretaceous Pierre Shale Formation. The term "marl" has long been used to describe the argillaceous chalky limestones and calcium carbonate-rich chalky shale

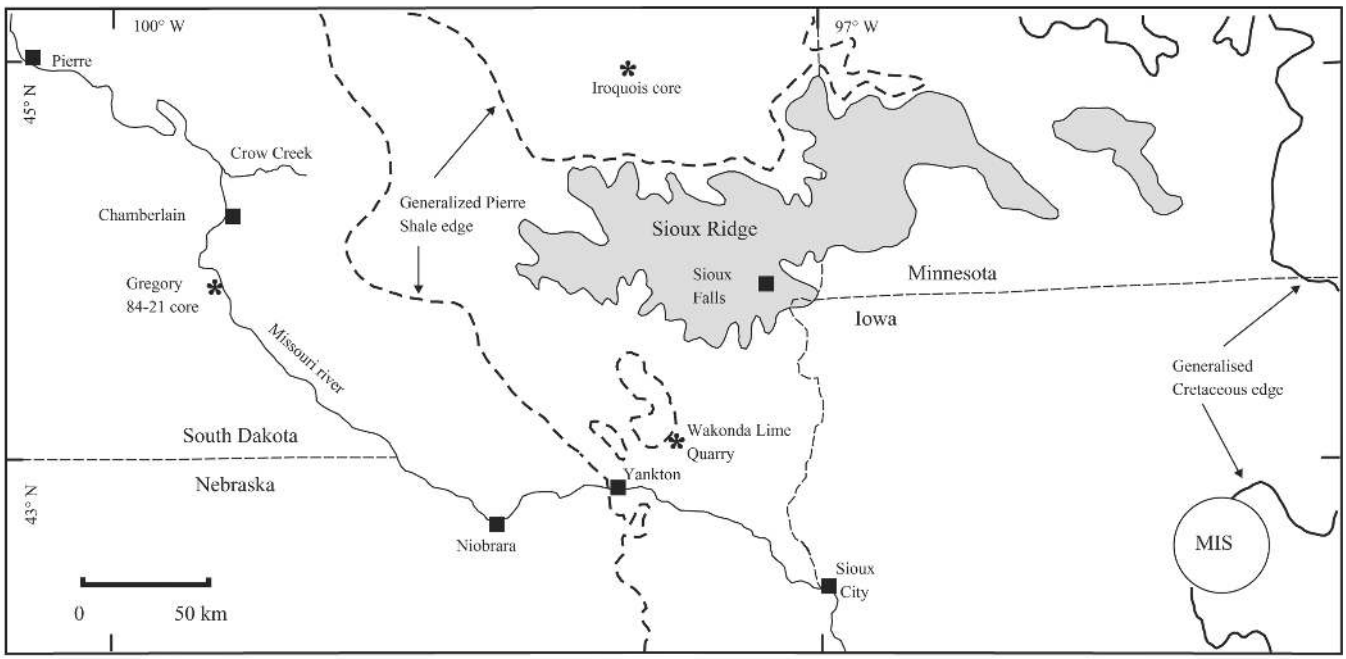

Fig. 1. Map of selected geologic features in the region encompassing the Missouri River Valley of southern South Dakota and adjacent Nebraska eastward to the Manson Impact Structure (MIS) of Iowa. Sample locations of Crow Creek strata are shown. Selected towns and cities marked by solid squares. Exposed region of Sioux Quartzite (shaded region) marks the topographically highest area of the Sioux Ridge (after Witzke et al. 1996).

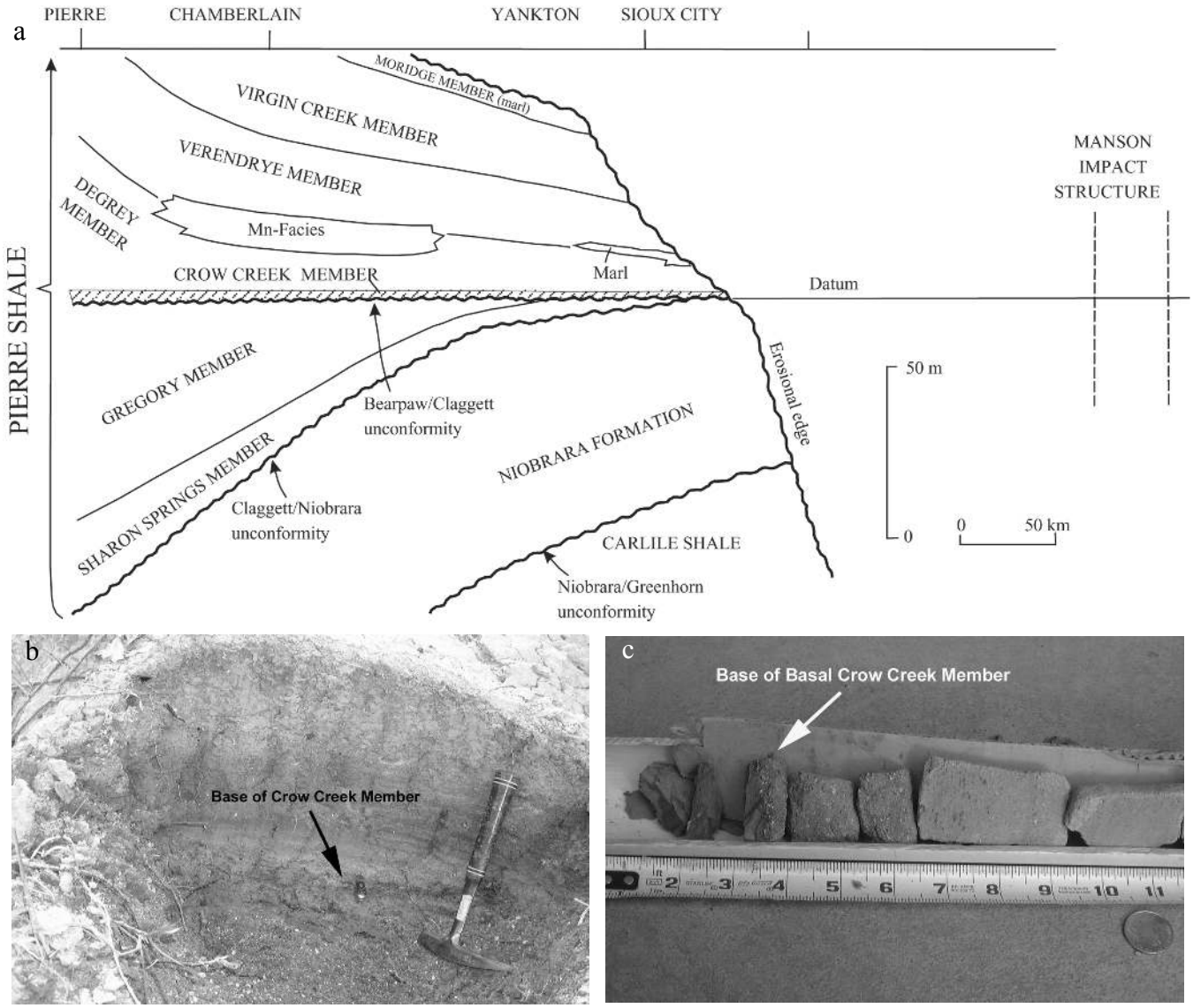

Fig. 2. a) General west-to-east stratigraphic cross section of Upper Cretaceous units in the study area. Datum is base of Crow Creek Member (cross-ruled interval). All units show general eastward thinning. Prominent regional unconformities are labeled. Approximate position of interval bearing manganese carbonate concretions is outlined in the upper DeGrey Member (Mn-facies) (after Witzke et al. 1996); b) field view of Wakonda Lime Quarry location. Knife is marking the base of the basal Crown Creek Member; c) basal Crow Creek Member in Gregory 84-21 core; tape is in inches.

units within the Pierre Shale. The Pierre Shale (type area in the Missouri River Valley near Pierre, South Dakota; Fig. 1) is a widespread shale-dominated marine interval of Campanian and lower Maastrichtian age that is recognized throughout the central and eastern area of the Cretaceous Western Interior Basin of North America. The intervals of calcareous shales and marls are restricted to eastern facies of the Pierre Shale, and are not present in the thicker western facies. The Pierre Shale is generally dark-colored shale of a maximum thickness of about 900 m. In the Missouri River valley of central South Dakota, the Pierre Shale is about 240 m thick and has been divided into eight members; in stratigraphic succession from the base, they are Sharon Springs, Gregory, Crow Creek, DeGrey, Verendrye, Virgin Creek, Mobridge (Fig. 2a) (Witzke et al. 1996).

The Crow Creek Member consists of 2–3 m of marl of which the lower 15 to 30 cm (the "basal unit") are sandy siltstone that is commonly cross-bedded (Izett et al. 1998). Like most members of the Pierre Shale, the Crow Creek tends to be thicker in the western than in the eastern areas (Crandell 1952; Schultz 1965; Bretz 1979). The basal sandy siltstone is the only bed of significant coarseness within the entire Pierre Shale. The basal contact is sharp and disconformable, and is marked by an abrupt lithologic change from dark claystone and shale to the calcareous, sandy siltstone. Rip-up shale clasts commonly are observed in the Crow Creek Member,

particularly in the lower part, and are most abundant in the southeastern exposures. The clasts are as large as 4 cm in size and resemble the immediately underlying members from which they have been derived.

The basal unit of the Crow Creek Formation (Figs. 2b and 2c) consists of silt-, sand-, and mudstone with a wackestone fabric, and contains scattered, granule-sized grains in a phosphatized argillaceous and calcareous mudstone matrix (Witzke et al. 1996). A remarkably high percentage of detrital quartz and feldspar grains in the basal clastic layer exhibit shock-induced features. Quartz is the dominant grain type, generally occurring as subangular to subrounded silt and sand grains. Most of the quartz is monocrystalline, but some polycrystalline grains, including chalcedony and chert, occur. Grain sizes range up to 4 mm. Feldspars, mainly orthoclase and rare plagioclase, occur in subordinate amounts relative to other components, which occur in appreciable amounts; these include detrital dolomite, shale clasts, sand- and siltstone, limestone clasts, calcite grains and abundant calcareous fossils. In some places, the basal Crow Creek layer is rich in phosphate material averaging about 9% by volume apatite, which also occur in underlying sediments. The clay fraction of the matrix is dominated by montmorillonite, with lesser amounts of kaolinite and illite. Compared to the basal unit, there is a general decrease in the relative proportions of impact-derived quartz in the marly unit (Witzke et al. 1996; Izett et al. 1998).

The Sioux Ridge, a paleo-topographic feature, is dominated by the very resistant Proterozoic Sioux Quartzite that was onlapped and mostly buried by Cretaceous strata (Fig. 1). It occupies a broad area of the subsurface across much of southeastern South Dakota trending from west of Pierre, southward into northeastern Nebraska and eastward into southwestern Minnesota and northwestern Iowa (Witzke et al. 1983; Anderson 1987), with the Sioux Quartzite presently exposed only along the highest portions of the ridge (Fig. 1). The distribution of Crow Creek strata is remarkably coincident with the subsurface extent of the Sioux Ridge, and all known occurrences of the member are recognized either directly above the Ridge or within about 50 km of the Sioux Quartzite edge (Witzke et al. 1996).

SAMPLE PREPARATION AND ANALYTICAL METHODS

Samples for this study were collected from the Crow Creek Member from Gregory 84-21 core (GC), Iroquois core (IC), and Wakonda lime quarry (WLQ) (Figs. 1, 2b, and 2c). Sample descriptions are presented in Table 1. Depths in meters reported here were converted from feet (ft) for Gregory and Iroquois drill core samples, and from centimeters (cm) for Wakonda lime quarry. Sample numbers represent sample depths e.g., Gregory core sample taken at 239.9 ft is sample GC239.9 corresponding to 73.14 m depth.

Weighed portions of gently crushed samples were soaked in water, stirred thoroughly and the turbid suspension (clay material <63 μm in size) decanted. This process was repeated several times until all the fines were removed. The residues were dissolved in hydrochloric acid (7 N HCl) and warmed on a hot plate to remove all carbonate minerals. The clay-free, acid insoluble residues were rinsed and dried in an oven at 110° for about 12 hours.

Iron oxides (especially in WLQ samples), zircon, and sphene were removed by heavy liquid separation method with lithium heteropolytungstate that has a density of 2.85 ± 0.02 g/ml. Quartz, feldspar, and micas with densities less than 2.85 g/ml floated in the heavy liquid and were recovered. Iron oxides and other dense minerals sunk to the bottom of the separating flask and were also recovered. The separated light and heavy minerals were thoroughly rinsed with acetone and dried at 110° for at least 2 hours.

Magnetic separation was done with the Franz isodynamic magnetic separator. The samples were separated at a current of 1.3A, 6° forward tilt and 5° side tilt. At these settings most of the strongly paramagnetic minerals were separated, leaving a concentrate of quartz and feldspar. The final residue was dried and screened with stacked 500 μm, 250 μm-, 125 μm-, and 63 μm- mesh sieves and resulting size fractions were weighed.

Each size fraction of felsic residues was examined by reflected light microscopy for shocked minerals. Shocked minerals i.e., those displaying PDFs, mostly quartz and rare feldspar were hand-picked from a few basal-unit samples (Table 2), mounted on glass slides in epoxy, and studied with an optical petrographic microscope. Crystallographic orientations of the PDFs in quartz were measured with a 4-axes universal stage mounted on a petrographic microscope stage. The angles between the PDFs and c-axes were determined by conventional stereographic plotting methods following procedures described by Engelhardt and Bertsch (1969) and plotted on histograms.

Contents of major elements and some trace elements including V, Cu, Sr, Y, and Nb were determined by standard X-ray fluorescence (XRF) procedures on powdered samples, following procedures described by Reimold et al. (1994). Rare earth elements (REE), Sc, Co, As, Se, Br, Sb, and Cs were determined by instrumental neutron activation analysis (INAA); see Koeberl (1993) for details of the methodology. All other elements were analyzed by both XRF and INAA. The amount of sample material was not enough for most IC samples for trace element analysis by XRF. For this reason, the contents of V, Cu, Sr, Y, and Nb were not analyzed in most IC samples (i.e., IC243.8, 243.6, 243.2, 242.8-243.0, 242.3-242.5, and 242.15-242.3).

RESULTS

The felsic contents in the samples vary from one sample suite to the other, with higher contents generally occurring in the basal-unit samples, ranging from 3–34 wt% (Table 2), but

Table 1. Descriptions of samples from the Crow Creek Member (samples are arranged from top to bottom).

Sample	Description
Gregory core 84-21 samples	
Marly layer GC236.28-236.0 (72.04–71.95 m) GC236.42 (72.08 m) GC236.56 (72.12 m) GC236.70 (72.16 m) GC236.84 (72.20 m) GC236.98 (72.24 m) GC237.12 (72.29 m) GC237.26 (72.34 m) GC237.40 (72.38 m) GC237.20-237.40 (72.32–72.38 m)	Gregory core samples consisted of half drill core pieces of the basal Crow Creek (BCC) and overlying marly layer. Marly layer samples (GC236.0-237.2) were of the same lithologic composition, being a light gray, massive calcareous mudstone, with no embedded coarser fragments. The samples span a thickness of 43 cm.
Basal unit GC239.9 (73.14 m)	The basal-unit sample (GC239.9) is lithologically different from the overlying marly samples. The sample was a piece of drill core, 3 cm in thickness. It was light-gray-colored, friable, silty sandy, calcareous mudstone, with numerous white sand-sized grains, with a thin 4 mm layer of dark gray mudstone.
Iroquois core (IC)	
Marly layer IC242.0-242.15 (73.78–73.83 m) IC242.15-242.3 (73.83–73.87 m) IC242.3-242.5 (73.87–73.93 m) IC242.5-242.8 (73.93–74.04 m) IC242.8 -243.0 (74.04–74.08 m)	The Iroquois core samples consist of BCC and overlying marly layer. The samples were drill core cuttings and represent a thickness of 55 cm.
Basal unit IC243.0 (74.04 m) (top) IC243.2 (74.15 m) IC243.4-243.6 (74.21–74.27 m) IC243.6 (74.27 m) IC243.8 (74.33 m) (bottom)	The marly layer samples (IC242.8-242.0) represent 30 cm thickness of the marl The samples are relatively light gray, hard, calcareous, silty mudstone, with a crude fine planar fabric defined by dark flaky minerals and flattened dark granules.
	The basal-unit samples (IC243.8-243.0) represent a thickness of 25 cm from the base. The samples were generally light gray colored, friable, composed of a silty-clay calcareous matrix, with sparsely distributed granules and shale fragments measuring 1–2 mm. The fragments embedded in a silty-clay matrix are composed of angular to subrounded of mainly dark gray shale. Other fragments are polycrystalline quartz and apatite. The bottom sample is dark gray marl, being calcareous with a mudstone texture and does not contain coarse grains or fragments.
Wakonda lime quarry (WLQ)	
Basal unit WLQ20-25 (+0.20–0.25 m) WLQ16-20 (+0.16–0.20 m) WLQ12-16 (+0.12–0.16 m) WLQ8-12 (+0.08–0.12 m) WLQ5-8 (+0.05–0.08 m) WLQ2-4 (+0.02–0.04 m) WLQ1 (+0.01 m) WLQ0 (bottom)	The samples represent the lower 25 cm unconformably overlying Pierre Shale. All the WLQ BCC samples (WLQ 0-20) were agglomerated loose brown weathered soil and composed of a mixture of silt and clay with granules of gray shale and white fragments. The brown color is due to iron oxides. All the samples fizzed vigorous with acid, indicating that they are calcareous and contain significant amounts of calcium carbonate.
Shale Pierre Shale: –2 (–0.02 m)	The Pierre shale sample (WLQ –2 cm) was taken 2 cm below the BCC and represents the enclosing Pierre shale. The Pierre Shale sample was also in loose form, and is calcareous, composed of a mixture of clay and fragments of shale.

Table 2. Amounts of quartz-feldspar (qtz-fsp) residues from initial amounts of Crow Creek Member samples.

Sample	Initial weight (g)	Qtz-fsp[a] (g)	Qtz-Fsp wt%	Shocked grains
Gregory 84-21 core				
Marly layer				
GC236.28-236.0 (72.04–71.95 m)	61.21	0.68	1.11	–
GC236.42 (72.08 m)	55.47	0.47	0.85	–
GC236.56 (72.12 m)	54.55	0.56	1.03	–
GC236.70 (72.16 m)	60.67	1.23	2.03	–
GC236.84 (72.20 m)	86.02	1.06	1.23	–
GC236.98 (72.24 m)	60.70	0.85	1.40	–
GC237.12 (72.29 m)	60.21	0.97	1.61	–
GC237.26 (72.34 m)	34.25	0.45	1.31	–
GC237.40 (72.38 m)	106.43	1.51	1.42	–
GC237.2-237.4 (72.32–72.38 m)	19.39	0.45	2.58	–
Basal unit				
GC239.90 (73. 14 m)	45.03	1.34	2.98	8 (qtz) 1 (fsp)
Iroquois core				
Marly layer				
IC242.0-242.15 (73.78–73.83 m)	8.06	0.22	2.73	–
IC242.15-242.3 (73.83–73.87 m)	7.17	0.43	5.58	–
IC242.3-242.5 (73.87–73.93 m)	7.27	0.17	2.34	–
IC242.5-242.8 (73.93–74.04 m)	6.67	0.22	3.33	–
IC242.8 -243.0 (74.04–74.08 m)	7.40	0.26	3.51	–
Basal unit				
IC243.0 (74.04 m) (top)	7.87	0.54	6.86	–
IC243.2 (74.15 m)	7.16	2.41	33.66	–
IC243.4 -243.6 (74.21–74.27 m)	9.82	1.83	18.64	–
IC243.6 (74.27 m)	7.33	1.71	23.33	1 (qtz) 1 (fsp)
IC243.8 (74.33 m) (bottom)	4.11	0.81	19.71	2 (qtz)
Wakonda lime quarry				
Basal unit				
WLQ20-25 (+0.20–0.25 m)	56.97	1.45	2.25	–
WLQ16-20 (+0.16–0.20 m)	54.30	2.94	5.41	–
WLQ12-16 (+0.12–0.16 m)	56.61	4.26	7.53	–
WLQ8-12 (+0.08–0.12 m)	40.48	3.33	8.23	1 (qtz)
WLQ5-8 (+0.05–0.08 m)	49.03	8.02	16.35	–
WLQ2-4 (+0.02–0.04 m)	42.89	8.25	19.24	–
WLQ1 (+0.01 m)	31.04	4.09	13.18	–
WLQ0 (bottom)	28.33	1.34	4.73	–
Shale				
Pierre Shale: –2 (–0.02 m)	16.84	0.43	2.55	–

[a]Felsic residue after removing fines (<63 μm size material), acid-soluble material, heavy and magnetic minerals.

there is no systematic gradational increase in felsic contents from the basal unit to the marly layer. The bulk of the felsic residue range in grain size from 125 to 250 μm.

Shock Petrography

The felsic residues contain mainly quartz and subordinate feldspars. Quartz consists mainly of clear angular grains and rare medium brown toasted grains. The feldspars are invariably altered to a turbid brown surface with barely discernible crosshatched twinning. Shocked minerals were rare and most were found in few samples, especially GC239.9 representing the basal unit of the Crow Creek Member (Table 2; Figs. 3a–3c) in the 125–250 μm size fractions. The shocked grains are subrounded to angular and display shock features such as PDFs and mosaicism. Most grains display PDFs up to 3 sets and rarely single sets. There was no objective way of estimating the relative abundances of the shocked minerals in the residues. A maximum number of ten shocked grains recovered from e.g., 0.25 g felsic residue of sample GC239.9 consisting of several

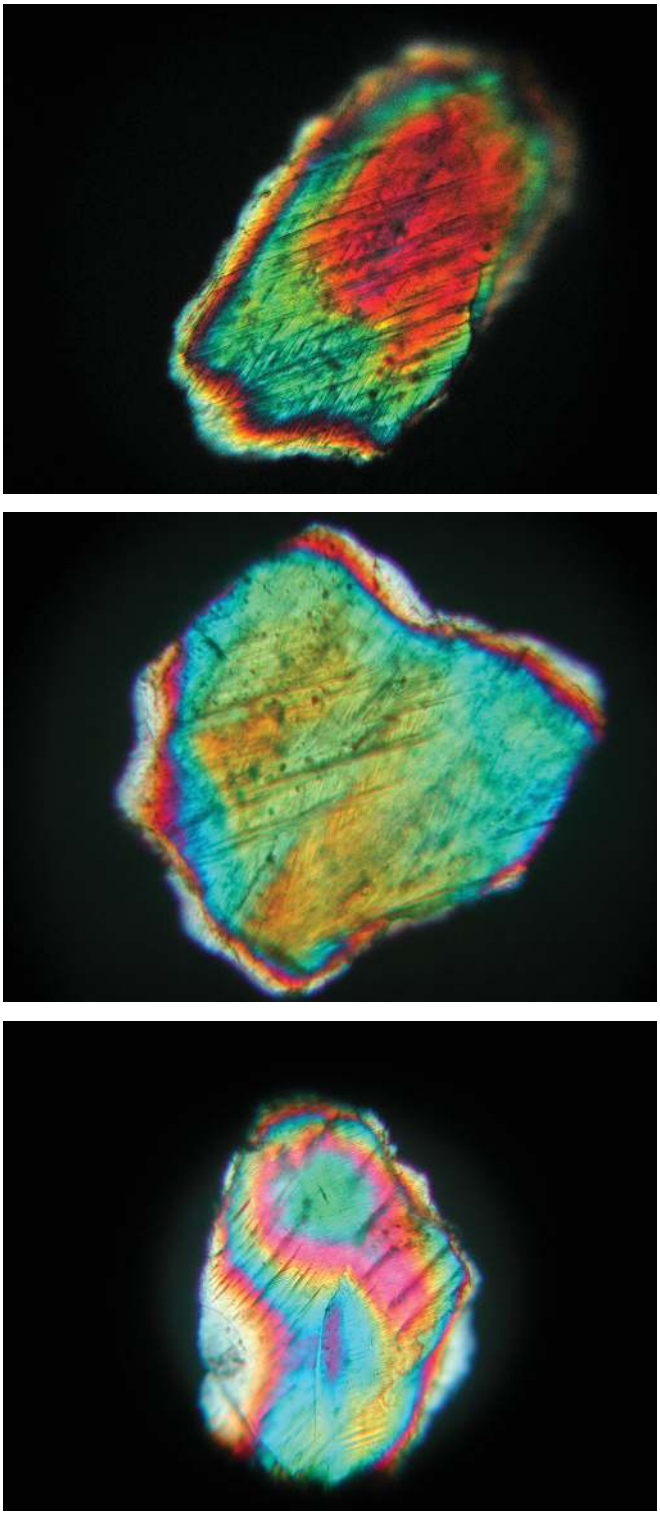

Fig. 3. Photomicrographs of some shocked quartz grains recovered from the Crow Creek Member displaying multiple sets of PDFs. Images taken in cross-polarized light: a) GC239.9; b) IC243.8; c) WLQ 8-12. Width of view is 175 mm. Images (a) and (b) show two sets of PDFs in this view, and more when rotated. Image (c) shows prominent subplanar fractures and two sets of much finer PDFs.

thousand grains, would represent <0.01 wt% of the material. The number of shocked minerals recovered in our samples is much lower than previously reported by Witzke et al. (1996) and Izett et al. (1998), probably due to the smaller amount of material available (<100 g/sample), compared to ~1000 g/sample used in their analyses or the uneven distribution of shocked material in ejecta.

The angles between the PDFs and c-axes, determined by conventional stereographic plotting methods following procedures described by Engelhardt and Bertsch (1969) show that the shock-characteristic orientation of $\{10\bar{1}3\}$ is dominant (Fig. 4a). PDF and c-axes orientations were compared with a standard stereographic projection of rational crystallographic planes in quartz (Engelhardt and Bertsch 1969; Stöffler and Langenhorst 1994), and results showed that 70% of the planes could be indexed. A plot of indexed planes according to Grieve and Therriault (1995) shows indexed shock-characteristic orientations of, ω, π, r, z, and s ($\{10\bar{1}3\}$, $\{10\bar{1}2\}$, $\{10\bar{1}1\}$, $\{01\bar{1}1\}$, and $\{11\bar{2}1\}$, respectively) (Fig. 4b). The relative frequency of the crystallographic orientations observed in the Crow Creek Member gives an indication that the shocked quartz in the Crow Creek Member were derived from target rocks, which were subjected to shock pressures of at least 15 GPa (French 1998).

Bulk Chemical Compositions

Major oxide and trace element contents of the samples from Crow Creek Member are presented in Tables 3a–3c and the ratios between them are summarized in Tables 4a–4c. Linear correlation coefficients between major-oxide and selected trace elements are given Table 5. The concentrations are compared with the composition of the Phanerozoic North American Shale Composite (NASC) (Gromet et al. 1984).

Major Elements

All the samples are composed mainly of SiO_2 (29–58 wt%), Al_2O_3 (6–14 wt%), and CaO (7–30 wt%), with varying amounts of the other oxides, reflecting the dominant mineralogical composition, which is mainly quartz, feldspar, carbonate, phosphate, and clay minerals. The CaO contents are rather low for true marl and carbonate rocks. Rocks with such contents of CaO are best referred to as marly or calcareous mudstones or shales. For this reason, the Crow Creek Member is referred to as a marly layer or loosely as marl. WLQ samples show relatively high SiO_2 contents compared to GC and IC samples. In WQL samples, SiO_2 shows a decreasing trend from the base (WLQ 0) to the top (WLQ 20). Harker variation diagrams show that SiO_2 has low positive correlations with Al_2O_3 ($r = +0.39$) and good negative correlations with CaO ($r = -0.87$) and to a lesser extent K_2O ($r = -0.63$) (Figs. 5a–5c). The contents of volatiles (LOI) are remarkably high, ranging from 13 to 42 wt%, due to abundant carbonate and organic material.

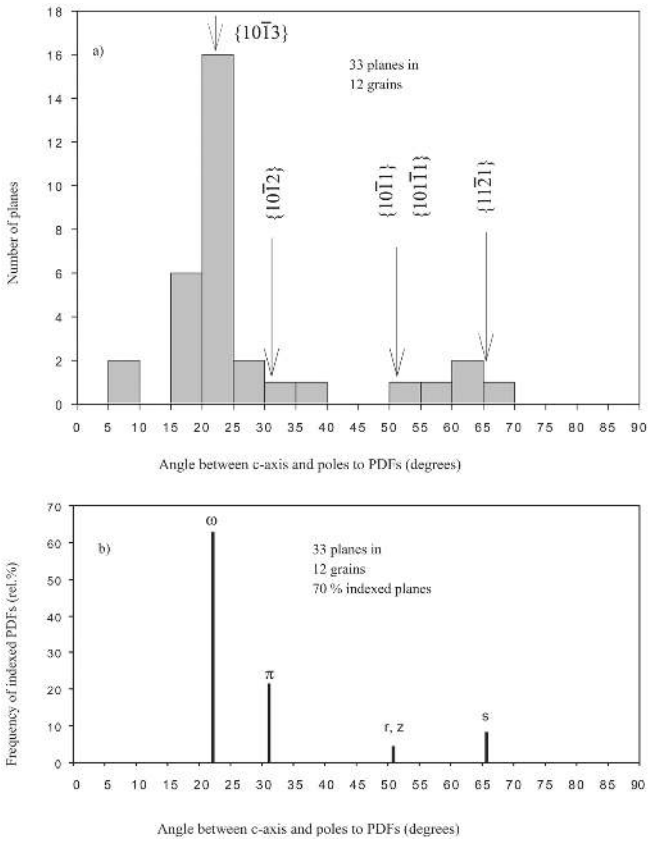

Fig. 4. Crystallographic orientations of PDFs in shocked quartz: a) Histogram showing angles between c-axis and PDFs plotted against frequency of PDF planes, for 33 planes in 12 grains; b) histogram showing angles between c-axis and PDFs plotted against frequency of 22 indexed PDF planes. The shock-characteristic orientations, {10$\bar{1}$3}, {10$\bar{1}$2}, {10$\bar{1}$1}, {01$\bar{1}$1}, and {11$\bar{2}$1} (ω, π, r, z, and s, respectively), are dominant.

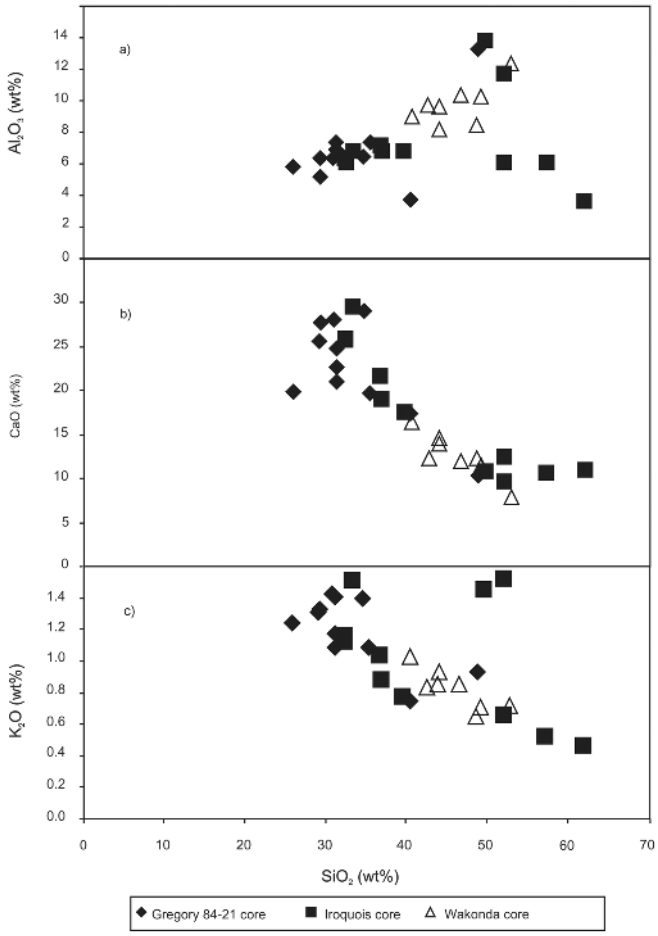

Fig. 5. Harker variation diagrams for the Crow Creek Member samples: a) Al_2O_3: weak positive linear correlation; b) CaO: good negative linear correlation; and c) K_2O: good negative linear correlation.

A plot of major elements normalized to NASC indicate moderate to significant depletions in SiO_2, Fe_2O_3, Al_2O_3, Na_2O and K_2O, and significant enrichments in CaO, MnO, and P_2O_5 (Figs. 6a–6c). The high contents of CaO and P_2O_5 are not surprising and are due to abundant carbonate and phosphate phases (Witzke et al. 1996). The Mn-facies in the Pierre Shale are common and explain the high MnO. The contents of Na_2O in the samples are variable and mostly low; some IC samples have contents below the detection limit of XRF.

Trace Elements

Trace element contents are quite uniform in each sample suite but show variations between the different sample suites. The contents are generally higher in the basal-unit samples.

Large Ion Lithophile Elements (LILE) and Transition Elements: The variations in the contents of LILE (Rb, Ba, Sr, Th, U) in each sample suite are low. Compared to the composition of NASC, Rb and Ba (except sample GC239.9) are depleted, while Sr and U are enriched (Figs. 8a–8c).

The abundances of transition elements (Cr, Co, Ni, Sc and V) are highly variable from one sample suite to the other (Figs. 7a–7c). Contents of Co and Sc are lower than those of Cr, Ni and V in all the samples. In the GC samples, all the metals especially V, are enriched in sample GC239.9, relative to the other samples where the contents are uniform. In the IC samples, Cr, Ni, and Sc are enriched in sample IC243.8 and IC243.6 compared to the other samples. Contents of Cr and V and to a lesser extent Ni are significantly high in WLQ samples, especially samples WLQ 5-8 and 8-12.

On the NASC-normalized diagrams (Figs. 8a–8c) Cr and Ni contents are slightly enriched in sample GC239.9 and IC243.4 and moderately in all the WLQ samples, while Co contents are either depleted or comparable to NASC. The contents of Sc are comparable to NASC in samples GC239.9 and WLQ samples, and lower in the other samples.

High Field Strength Elements (HFSE): High field strength elements (e.g., Zr, Nb, Hf, Ta, Y, Th, and U) and REE are enriched in felsic rather than mafic rocks and are thus very

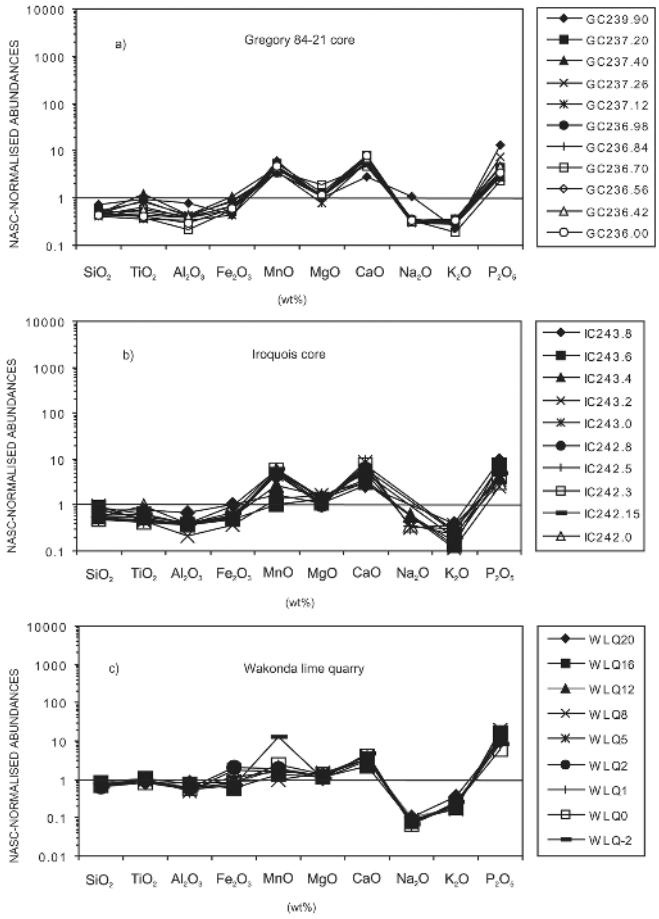

Fig. 6. North American Shale Composite (NASC)-normalized (Gromet et al. 1984) diagrams of major elements for the Crow Creek Member samples: a) Gregory 84-21 core; b) Iroquois core; and c) Wakonda lime quarry.

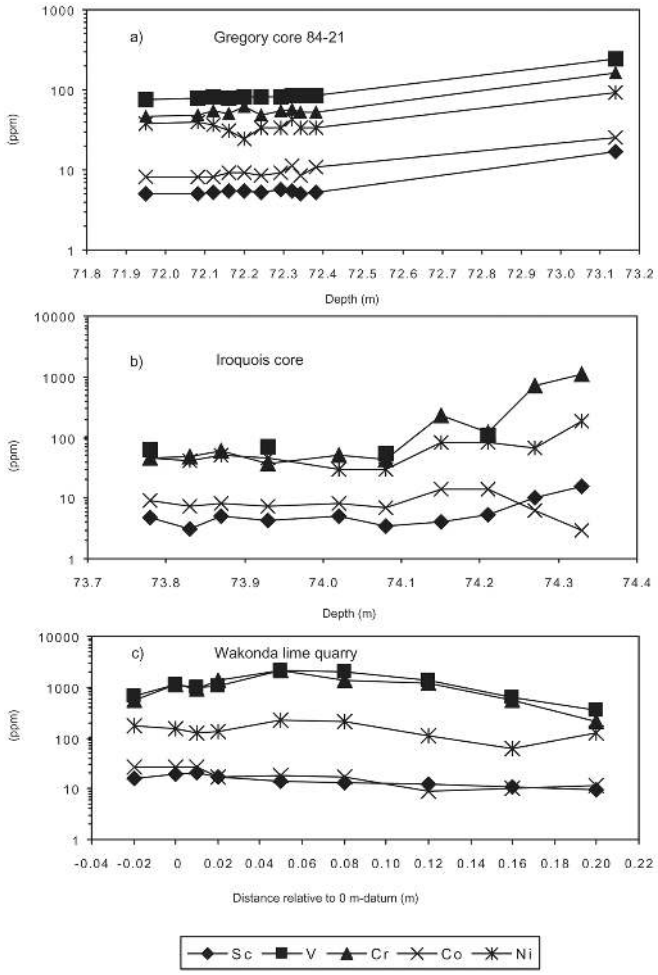

Fig. 7. Plot of contents of Cr, Co, Ni, Sc, and V in the Crow Creek Member samples showing variations with depth: a) Gregory 84-21 core; b) Iroquois core; and c) Wakonda lime quarry.

useful discriminants for provenance compositions (Taylor and McLennan 1985). Compared to element abundances in NASC, all the samples are significantly enriched in Y by up to two orders of magnitude, while U enrichment is moderate (Figs. 7a–7c). The contents of Zr, U, and Ta are slightly depleted in GC and IC, but the average contents in WLQ are comparable to NASC.

The abundances of Th and U are almost equal, as indicated by the Th/U ratios, which range from 0.6 to 1.10, except for one sample (GC239.9 = 4.71). The Th/U ratios in the samples are markedly higher than that of NASC (0.22), but lower than that of upper continental crust (3.8) (Taylor and McLennan 1985).

Rare Earth Elements (REE): Chondrite-normalized (Taylor and McLennan 1985) REE distribution patterns are presented in Figs. 9a–9c. All the samples are enriched in both light rare earth elements (LREE) and heavy rare earth elements (HREE) relative to chondritic contents, and show very uniform fractionated patterns with (La_N/Yb_N) values ranging from 6.02 to 9.49. The patterns are typical of shale and comparable with that of NASC. The distribution patterns have moderately fractionated LREE (La_N/Sm_N = 3.13–3.99; flat HREE (Gd_N/Yb_N = 1.24–1.84); and slight negative Eu-anomalies (Eu/Eu* = 0.54–0.75).

Total REE contents are relatively higher in the samples taken from basal units compared to upper overlying marly samples (GC239.9: basal: 632 ppm; upper: 100 ppm; IC243.8: basal: 248 ppm; upper: 75 ppm; and WLQ 1: basal: 613 ppm; upper: 124 ppm). Relative to NASC, REE contents are marginally lower in the GC and IC (except 2 samples, IC243.6 and IC 243.8) and variably higher in the WLQ samples.

DISCUSSION

Bulk Chemical Compositions

The ratio of K_2O-Al_2O_3 is important in sedimentary rocks in understanding the source of Al and its distribution between clay and feldspars minerals. The ratio of K_2O-Al_2O_3 of clay minerals and feldspars is markedly different. Values for clay minerals range from 0.0 to 0.3 and those for feldspars

Table 3a. Chemical compositions of the Crow Creek Member samples: Gregory 84-21 core (GC).[a]

Unit	Basal unit	Marly layer									
Sample	GC239.9	GC237.2 –237.4	GC237.40	GC237.26	GC237.12	GC236.98	GC236.84	GC236.70	GC236.56	GC236.42	GC236.28 –236.0
Depth (m)	73.14	72.32 –72.38	72.38	72.34	72.29	72.24	72.20	72.16	72.12	72.08	72.04 –71.95
SiO_2	48.79	34.62	31.20	35.41	25.88	31.17	30.86	40.40	29.19	31.28	29.30
TiO_2	0.76	0.38	0.93	0.67	0.29	0.68	0.35	0.31	0.49	0.43	0.33
Al_2O_3	13.28	6.49	7.38	7.36	5.86	6.89	6.34	3.71	6.33	6.79	5.20
Fe_2O_3	2.51	3.20	6.05	4.85	2.58	5.18	3.28	3.19	3.96	3.72	3.38
MnO	0.38	0.32	0.27	0.21	0.22	0.21	0.25	0.22	0.26	0.27	0.29
MgO	2.83	3.72	3.32	3.16	2.24	3.24	3.16	5.65	3.13	3.09	3.26
CaO	10.40	29.10	21.01	19.77	19.96	22.60	28.17	17.39	25.70	24.87	27.69
Na_2O	1.23	0.40	0.40	0.34	0.38	0.41	0.39	0.40	0.37	0.36	0.38
K_2O	0.93	1.40	1.09	1.09	1.24	1.17	1.43	0.75	1.31	1.41	1.33
P_2O_5	1.46	0.49	0.32	0.83	0.33	0.32	0.41	0.25	0.35	0.52	0.37
LOI	16.39	19.04	26.96	26.85	41.37	27.08	24.87	27.31	27.60	27.62	27.68
Total	98.96	99.16	98.93	100.54	100.35	98.95	99.51	99.58	98.69	100.36	99.21
Sc	17.0	5.25	5.00	5.43	5.67	5.18	5.53	5.49	5.15	5.10	4.98
V	242	86	86	84	83	82	82	78	81	78	75
Cr	162	53	53	56	54	49	62	51	54	48	47
Co	25.0	10.7	8.35	11.4	9.36	8.47	9.19	9.22	8.29	8.25	8.03
Ni	94	34	33	42	33	34	25	31	36	40	38
Cu	66	20	22	22	20	19	21	20	20	20	19
Zn	1267	56	55	54	54	62	51	58	54	62	75
As	<0.5	15.8	15.9	16.9	16.9	18.7	15.3	16.5	17.6	15.2	17.3
Se	5.27	4.34	4.46	4.82	4.68	4.42	4.62	4.22	4.4	4.03	4.42
Br	0.2	1.6	1.4	1.7	1.6	<1	1.5	1.4	2.8	3.8	<1.3
Rb	35	52	53	53	56	53	54	55	50	51	50
Sr	453	859	871	839	855	833	853	842	828	839	782
Y	180	20	25	25	23	27	26	21	24	21	25
Zr	261	134	155	147	128	122	126	138	127	127	147
Nb	20	4	5	5	5	5	4	4	5	4	5
Sb	0.13	2.93	2.77	3.5	2.99	2.02	2.76	3.09	1.83	1.77	1.93
Cs	1.4	3.33	3.26	3.86	3.77	3.11	3.62	3.7	3.02	2.98	2.87
Ba	1357	250	248	300	250	276	259	246	244	248	309
La	124	26.5	26.4	27.8	28.8	28.9	26.5	28.1	26.4	26.8	27.7
Ce	242	42.9	42.4	44.4	48.3	43.5	45.0	45.3	40.5	40.0	41.5
Nd	163	23.6	23.8	25.2	25.1	24	23.7	24.1	22.5	21.6	24.0
Sm	40.7	4.72	4.68	5.25	5.44	5.06	4.69	5.01	4.58	4.34	4.95
Eu	8.36	1.09	0.97	1.05	1.09	1.06	1.21	1.18	0.97	0.97	1.00
Gd	33.9	4.2	4.35	4.20	5.08	4.88	4.60	4.81	3.69	3.52	3.86
Tb	5.52	0.64	0.72	0.79	0.91	0.80	0.76	0.76	0.65	0.57	0.71
Tm	1.67	0.34	0.32	0.43	0.47	0.39	0.32	0.3	0.32	0.28	0.35
Yb	11.5	2.25	2.28	2.28	2.30	2.18	2.10	2.02	1.97	1.95	2.30
Lu	1.59	0.33	0.34	0.38	0.32	0.37	0.33	0.32	0.32	0.30	0.32
Hf	5.53	2.35	2.55	2.65	2.79	2.84	2.48	2.56	2.44	2.56	2.75
Ta	1.38	0.59	0.52	0.61	0.63	0.54	0.59	0.65	0.49	0.52	0.49
W	0.39	0.98	0.72	0.68	1.62	1.35	0.67	0.9	1.03	<0.61	0.56
Ir (ppb)	1.6	1.6	2.4	<2	<2	<1	1.1	0.9	0.6	0.4	<1
Au (ppb)	0.73	0.65	0.33	0.48	0.23	0.32	0.21	1.08	0.71	0.3	0.85
Th	19.6	5.53	5.3	6.2	6.25	6.00	5.6.0	5.87	5.44	5.16	5.59
U	4.16	4.69	4.77	6.30	5.93	7.17	4.84	5.37	5.23	5.27	6.80
CIA’	81	75	80	81	75	78	74	72	76	76	72
CIW’	87	91	92	93	90	91	91	85	91	92	89

[a]Major-oxide elements in wt%, trace elements in ppm except as noted; all Fe as Fe_2O_3; LOI: Loss on ignition; CIA’ = molar $(Al_2O_3/(Al_2O_3+Na_2O+K_2O)*100)$; CIW’ = molar $(Al_2O_3/(Al_2O_3+Na_2O)*100)$

Table 3b. Chemical compositions of the Crow Creek Member samples: Iroquois core (IC).[a]

Unit	Basal unit				Marly layer					
Sample	IC243.8	IC243.6	IC243.4 –242.6	IC243.2	IC243.0	IC242.8 –243.0	IC242.5 – 242.8	IC242.3 –242.5	IC242.15 –242.3	IC242.0 –242.15
Depth (m)	74.33	74.27	74.21 –74.27	74.15	74.08	74.02 –74.08	73.87 –74.02	73.83 –73.93	73.83 –73.93	73.78 –73.83
SiO_2	51.95	57.17	51.94	61.88	33.28	36.65	32.32	32.40	39.59	36.80
TiO_2	0.62	0.48	0.41	0.36	0.38	0.44	0.35	0.33	0.51	0.77
Al_2O_3	11.77	6.05	6.06	3.64	6.84	7.20	6.32	6.12	6.86	6.79
Fe_2O_3	5.87	2.69	3.11	2.06	3.41	2.81	2.78	2.98	3.86	5.65
MnO	0.10	0.06	0.16	0.08	0.27	0.28	0.33	0.35	0.36	0.35
MgO	3.13	3.94	4.31	4.86	3.16	2.98	2.77	3.15	4.02	3.77
CaO	9.74	10.64	12.47	10.95	29.59	21.67	25.75	25.90	17.56	19.04
Na_2O	<0.01	<0.01	0.68	<0.01	0.38	<0.01	0.39	<0.01	<0.01	0.41
K_2O	1.52	0.52	0.66	0.47	1.51	1.04	1.16	1.12	0.78	0.88
P_2O_5	1.00	0.85	0.45	0.28	0.40	0.76	0.48	0.47	0.54	0.33
LOI	13.09	16.16	18.45	15.89	21.30	26.39	26.53	26.18	24.60	24.76
Total	98.79	98.56	98.70	100.47	100.52	100.22	99.18	99.00	98.68	99.55
Sc	15.4	10.4	5.44	4.09	3.46	5.07	4.38	5.10	3.08	4.82
V	n.d	n.d	106	n.d	54	n.d	70	n.d	n.d	63
Cr	1083	713	124	229	44	50	37	59.4	47.8	47
Co	2.94	6.37	14.0	13.7	6.94	8.01	7.25	8.29	7.41	9.31
Ni	186	65.9	81	85	29	30.2	47	52.1	40.9	46
Cu	n.d	n.d	14	n.d	10	n.d	17	n.d	n.d	16
Zn	61.2	176	346	39.0	139	65.6	69.0	76.2	38.9	62.0
As	10.6	10.3	11.9	11	20.3	17.6	14.2	17.6	17.8	18.6
Se	4.58	5.21	2.15	3.47	4.04	3.41	2.75	3.29	2.4	2.82
Br	<2	0.9	2.2	1.8	1.7	4.5	3.3	4.4	2.9	3.3
Rb	81.3	13.5	27.0	14.8	21.0	45.8	44	42.9	23.3	46.0
Sr	n.d	n.d	374	n.d	280	n.d	897	n.d	n.d	710
Y	n.d	n.d	26	n.d	20	n.d	17	n.d	n.d	22
Zr	357	329	138	230	227	123	132	185	184	158
Nb	n.d	n.d	9	n.d	8	n.d	3	n.d	n.d	4
Sb	2.14	2.07	2.37	1.38	2.53	1.74	1.62	1.98	1.51	2.09
Cs	5.41	0.79	1.26	0.55	0.93	3.09	2.47	2.94	1.28	2.57
Ba	376	461	143	155	123	161	155	178	330	141
La	60.7	57.1	22.3	21.9	21.8	23.3	21.1	25.3	18.2	25.0
Ce	95.5	90.0	38.4	36.1	37.6	39.0	35.9	40.0	30.1	40.0
Nd	54.6	47.6	20.8	19.2	21.8	17.3	18.5	20.3	17.1	21.2
Sm	12.2	11.3	4.25	4.03	4.19	3.89	3.33	4.17	3.45	4.12
Eu	2.73	2.58	0.96	0.88	0.91	0.85	0.83	0.90	0.69	0.88
Gd	10.9	10.9	4.80	4.04	3.87	3.76	3.44	3.56	2.73	3.86
Tb	1.96	1.81	0.82	0.69	0.66	0.56	0.49	0.63	0.49	0.65
Tm	1.08	0.93	0.34	0.38	0.36	0.29	0.22	0.32	0.28	0.29
Yb	6.69	6.36	2.22	2.46	2.25	1.66	1.58	1.84	1.78	1.78
Lu	1.17	0.91	0.35	0.35	0.36	0.28	0.22	0.33	0.28	0.29
Hf	5.48	4.71	3.78	5.28	6.33	2.99	2.88	3.46	4.04	3.27
Ta	1.07	1.06	0.59	0.55	0.42	0.77	0.75	0.5	0.36	0.49
W	<2	<1	<1	2.6	0.9	1.4	<1	<1	<1	2.0
Ir (ppb)	0.6	<2	1.2	<2	<2	<2	<1	<2	1.1	<2
Au (ppb)	1.79	0.98	0.62	0.25	0.13	0.13	0.18	0.35	0.11	0.7
Th	13.0	9.97	6.08	4.83	5.04	5.49	4.63	5.10	5.24	5.33
U	13.4	10.9	5.73	4.29	5.96	6.32	5.55	8.1	5.13	6.96
CIA’	88	91	77	88	75	86	77	83	89	81
CIW’	>99	>99	84	>99	92	>99	91	>99	>99	91

[a]Major-oxide elements in wt%, trace elements in ppm except as noted; all Fe as Fe_2O_3; n.d: not determined; LOI: Loss on ignition; CIA’ = molar $(Al_2O_3/(Al_2O_3+Na_2O+K_2O)*100)$; CIW’ = molar $(Al_2O_3/(Al_2O_3+Na_2O)*100)$.

Table 3c. Chemical compositions of the Crow Creek Member samples: Wakonda lime quarry (WLQ).[a]

Unit	Pierre Shale	WLQ basal-unit							
Sample	WLQ-2	WLQ0	WLQ1	WLQ2-4	WLQ5-8	WLQ8-12	WLQ12-16	WLQ16-20	WLQ20-25
Depth (m)	−0.02	0	0.01	0.02–0.04	0.05–0.08	0.08–0.12	0.12–0.16	0.16–0.20	0.20–0.25
SiO_2	49.63	52.85	49.13	48.53	43.95	42.60	46.56	43.99	40.57
TiO_2	0.66	0.82	0.89	0.79	0.77	0.75	0.78	0.65	0.64
Al_2O_3	13.86	12.36	10.29	8.45	8.22	9.74	10.39	9.66	8.96
Fe_2O_3	4.56	3.33	4.38	5.21	9.75	12.10	6.82	4.76	4.03
MnO	0.11	0.08	0.14	0.06	0.10	0.11	0.10	0.15	0.80
MgO	2.90	3.39	3.83	4.11	3.75	3.52	3.91	3.95	3.14
CaO	10.86	7.85	11.49	12.28	13.96	12.38	11.98	14.64	16.48
Na_2O	0.12	0.09	0.12	0.10	0.09	0.10	0.08	0.08	0.08
K_2O	1.45	0.72	0.71	0.65	0.85	0.83	0.85	0.93	1.03
P_2O_5	1.14	1.83	1.91	2.13	1.47	1.30	0.99	0.68	0.94
LOI	13.78	15.45	16.05	17.39	16.44	16.84	17.83	20.85	23.10
Total	99.07	98.77	98.94	99.70	99.35	100.27	100.29	100.34	99.77
Sc	16.4	21.3	18.8	17.5	14.0	13.4	12.1	10.6	9.23
V	665	1016	1108	1053	2102	2039	1399	640	359
Cr	536	928	1146	1374	2086	1321	1195	550	207
Co	27.1	27.0	27.0	6.72	18.1	17.5	8.78	10.4	11.6
Ni	178	128	156	131	231	214	112	60	122
Cu	49	37	41	36	30	35	22	22	33
Zn	379	422	296	265	422	363	160	98	64
As	12.6	<2	4.5	24	48	48	26	18	23
Se	4.81	5.08	4.39	4.18	5.16	4.66	3.91	4.86	3.65
Br	6.9	27	22	<2	10	8.9	4.9	3.4	2.7
Rb	68	28	24	22	27	26	31	34	42
Sr	220	291	196	295	235	226	240	343	484
Y	197	216	210	186	116	77	59	40	26
Zr	253	243	242	214	221	253	182	180	148
Nb	31	38	33	25	29	29	27	26	23
Sb	3.37	47.9	2.97	2.23	5.54	4.29	2.34	1.67	1.43
Cs	4.41	1.25	1.25	2.23	1.33	1.20	1.45	1.90	2.40
Ba	278	276	226	236	270	264	162	128	130
La	124	144	168	158	100	64.5	58.5	37.7	29.0
Ce	156	194	231	211	138	95.5	92.8	65.1	51.8
Nd	96.7	118	133	126	89.1	58.8	53.4	33.9	26.0
Sm	22.0	27.2	28.8	28.7	19.4	12.5	11.5	7.54	5.44
Eu	5.35	5.78	6.85	6.61	4.26	2.76	2.45	1.30	0.98
Gd	22.2	20.9	23.9	27.2	19.2	11.8	10.4	7.23	5.70
Tb	3.78	3.95	4.60	4.38	3.06	1.81	1.85	1.06	0.97
Tm	2.17	1.82	2.29	2.2	1.29	0.92	0.95	0.56	0.5
Yb	13.1	12.6	12.8	13.1	8.61	5.97	5.41	3.48	3.24
Lu	2.14	2.26	2.17	2.00	1.50	0.95	0.84	0.58	0.46
Hf	6.57	6.7	6.24	5.41	5.76	6.07	4.44	5.32	4.27
Ta	1.23	1.58	1.56	1.66	2.09	2.24	2.55	1.73	1.32
W	<1	<2	7.5	<2	5.5	<1	<1	6.2	3.7
Ir (ppb)	0.9	<4	0.5	<2	<2	<2	<3	<7	0.6
Au (ppb)	2.89	2.36	3.51	3	2.3	0.97	2.00	0.72	3.00
Th	16.5	19.7	17.9	17.8	17.3	14.6	15.4	12.5	9.08
U	18.0	28.5	25.6	29.9	25.4	15.5	11.6	10.1	7.78
CIA’	89	93	91	91	88	90	91	89	88
CIW’	99	99	98	98	98	98	99	99	99

[a]Major-oxide elements in wt%, trace elements in ppm except as noted; all Fe as Fe_2O_3; LOI: Loss on ignition; CIA’ = molar $(Al_2O_3/(Al_2O_3+Na_2O+K_2O)*100)$; CIW’ = molar $(Al_2O_3/(Al_2O_3+Na_2O)*100)$.

Table 4a. Element ratios of Gregory 84-21 core samples (GC).

Unit	Basal unit	Marly layer									
Sample	GC239.9	GC237.2 –237.4	GC237.4	GC237.26	GC237.12	GC236.98	GC236.84	GC236.7	GC236.56	GC236.42	GC236.28 –236.0
Depth (m)	73.14	72.32 –72.38	72.38	72.34	72.29	72.24	72.20	72.16	72.12	72.08	72.04 –71.95
K/U	1856	2478	1897	1436	1736	1354	2452	1159	2079	2221	1623
Cr/Th	8	10	10	9	9	8	11	9	10	9	8
Th/Sc	1.15	1.05	1.06	1.14	1.10	1.16	1.01	1.07	1.06	1.01	1.12
La/Sc	7.29	5.05	5.28	5.12	5.08	5.58	4.79	5.12	5.13	5.25	5.56
Sc/Th	0.87	0.95	0.94	0.88	0.91	0.86	0.99	0.94	0.95	0.99	0.89
Co/Th	1.28	1.93	1.58	1.84	1.50	1.41	1.64	1.57	1.52	1.60	1.44
La/Co	4.96	2.48	3.16	2.44	3.08	3.41	2.88	3.05	3.18	3.25	3.45
Th/Co	0.78	0.52	0.63	0.54	0.67	0.71	0.61	0.64	0.66	0.63	0.70
Zr/Hf	47	57	61	55	46	43	51	54	52	50	53
La/Th	6.33	4.79	4.98	4.48	4.61	4.82	4.73	4.79	4.85	5.19	4.96
Th/U	4.71	1.18	1.11	0.98	1.05	0.84	1.16	1.09	1.04	0.98	0.82
La_N/Sm_N	1.92	3.53	3.55	3.33	3.33	3.59	3.56	3.53	3.63	3.89	3.52
La_N/Yb_N	7.29	7.96	7.82	8.24	8.46	8.96	8.53	9.40	9.06	9.29	8.14
Gd_N/Yb_N	2.39	1.51	1.55	1.49	1.79	1.81	1.78	1.93	1.52	1.46	1.36
Eu/Eu[a]	0.69	0.75	0.66	0.68	0.63	0.65	0.80	0.73	0.72	0.76	0.70

[a]$Eu/Eu^* = Eu_N/(Sm_N \times Gd_N)^{0.5}$.

Table 4b. Element ratios of Iroquois core samples (IC).

Unit	Basal unit				Marly layer					
Sample	IC243.8	IC243.6	IC243.4 –242.6	IC243.2	IC243.0	IC242.8 –243.0	IC242.5 –242.8	IC242.3 –242.5	IC242.15 –242.3	IC242.0 –242.15
Depth (m)	74.33	74.27	74.21 –74.27	74.15	74.08	74.02 –74.08	73.87 –74.02	73.83 –73.93	73.83 –73.93	73.78 –73.83
K/U	941	396	956	909	2103	1366	1735	1148	1262	1049
Cr/Th	83	72	20	47	9	9	8	12	9	9
Th/Sc	0.84	0.96	1.12	1.18	1.46	1.08	1.06	1.00	1.70	1.11
La/Sc	3.94	5.49	4.10	5.35	6.30	4.60	4.82	4.96	5.91	5.19
Sc/Th	1.18	1.04	0.89	0.85	0.69	0.92	0.95	1.00	0.59	0.90
Co/Th	0.23	0.64	2.30	0.28	1.38	1.46	1.57	1.63	1.41	1.75
La/Co	20.65	8.96	1.59	15.99	3.14	2.91	2.91	3.05	2.46	2.69
Th/Co	4.42	1.57	0.43	3.53	0.73	0.69	0.64	0.62	0.71	0.57
Zr/Hf	65	70	37	44	36	41	46	53	46	48
La/Th	4.67	5.73	3.67	4.53	4.33	4.24	4.56	4.96	3.47	4.69
Th/U	0.97	0.91	1.06	1.13	0.85	0.87	0.83	0.63	1.02	0.77
La_N/Sm_N	3.13	3.18	3.30	3.42	3.27	3.77	3.99	3.82	3.32	3.82
La_N/Yb_N	6.13	6.07	6.79	6.02	6.55	9.48	9.02	9.29	6.91	9.49
Gd_N/Yb_N	1.32	1.39	1.75	1.33	1.39	1.84	1.76	1.57	1.24	1.76
Eu/Eu[a]	0.72	0.71	0.65	0.67	0.69	0.68	0.75	0.71	0.69	0.67

[a]$Eu/Eu^* = Eu_N/(Sm_N \times Gd_N)^{0.5}$.

from 0.3 to 0.9 (Cox et al. 1995). In the Crow Creek samples, the ratio ranges from 0.07 to 0.27 indicating that clay minerals have a major role in the distribution of Al in these rocks.

Yttrium, Zr, Nb, and Th have variable positive correlations coefficients with P_2O_5 (r = +0.90, +0.55, +0.91 and +0.88), respectively. Correlations of these elements are equally variable with SiO_2 (r = +0.75, +0.73, +0.81, and +0.60) and Al_2O_3 (r = +0.79, +0.54, +0.82, and +0.83), respectively. The higher positive correlations between Y and Th, and P_2O_5 suggest that the abundances of these elements are chiefly controlled by the presence of phosphates. The significant positive correlation between Zr and SiO_2 indicates that Zr abundance is controlled by zircon. Niobium contents correlate well with transition elements, REE, Y, and Th (r = >+0.80), while Thorium shows a good correlation with Sc (r = +0.91), indicating that these elements are partitioned in different minerals or compounds.

Provenance

Here, we attempt to discuss possible bulk chemical compositions of the source rocks for the Crow Creek strata using major and trace element chemistry.

Evidence from Major Elements

In an attempt to infer the provenance of material using major element compositions, we employed the discriminant function diagram of Roser and Korsch (1998) (Fig. 10). The

Table 4c. Element ratios of Wakonda lime quarry samples (WLQ).

Unit	Pierre shale	WLQ Basal-unit							
Sample	WLQ-2	WLQ0	WLQ1	WLQ2-4	WLQ5-8	WLQ8-12	WLQ12-16	WLQ16-20	WLQ20-25
Depth (m)	–0.02	0	0.01	0.02–0.04	0.05–0.08	0.08–0.12	0.12–0.16	0.16–0.20	0.20–0.25
K/U	669	210	230	180	278	444	608	764	1099
Cr/Th	32	47	64	77	121	90	78	44	23
Th/Sc	1.01	0.92	0.95	1.02	1.24	1.09	1.27	1.18	0.98
La/sc	7.56	6.76	8.94	9.03	7.14	4.81	4.83	3.56	3.14
Sc/Th	0.99	1.08	1.05	0.98	0.81	0.92	0.79	0.85	1.02
Co/Th	1.64	1.37	1.51	0.38	1.05	1.20	0.57	0.83	1.28
La/Co	4.58	5.33	6.22	23.51	5.52	3.69	6.66	3.63	2.50
Th/Co	0.61	0.73	0.66	2.65	0.96	0.83	1.75	1.20	0.78
Zr/Hf	39	36	39	40	38	42	41	34	35
La/Th	7.52	7.31	9.39	8.88	5.78	4.42	3.80	3.02	3.19
Th/U	0.92	0.69	0.70	0.60	0.68	0.94	1.33	1.24	1.17
La_N/Sm_N	3.55	3.33	3.67	3.47	3.24	3.25	3.20	3.15	3.36
La_N/Yb_N	6.40	7.72	8.87	8.15	7.85	7.30	7.31	7.32	6.05
Gd_N/Yb_N	1.37	1.34	1.51	1.68	1.81	1.60	1.56	1.68	1.43
Eu/Eu[a]	0.74	0.74	0.80	0.72	0.67	0.69	0.68	0.54	0.54

[a]$Eu/Eu^* = Eu_N/(Sm_N \times Gd_N)^{0.5}$.

Table 5. Linear correlation coefficients (r) between major oxide and selected trace elements of data in Table 3.

SiO_2	TiO_2	Al_2O_3	Fe_2O_3	MgO	CaO	Na_2O	K_2O	P_2O_5	Sc	Cr	Co	Y	Zr	Nb	La	Yb	Th	
SiO_2	–	0.33	0.39	0.05	0.49	–0.87	–0.14	–0.65	0.53	0.61	v0.53	0.28	0.75	0.73	0.81	0.53	0.60	v0.60
Sc	0.61	0.66	0.83	0.33	–0.02	–0.74	–0.27	–0.27	0.92	–	0.76	0.69	0.95	0.67	0.93	0.93	0.95	0.97
V	0.57	0.57	0.50	0.79	0.20	–0.63	–0.55	–0.51	0.72	0.70	0.97	0.45	0.54	0.66	0.81	0.59	0.59	0.76
Cr	0.53	0.58	0.49	0.68	0.18	–0.63	–0.56	–0.36	0.77	0.76	–	0.34	0.61	0.59	0.80	0.69	0.69	0.79
Co	0.28	0.51	0.69	0.18	–0.15	–0.43	0.00	–0.13	0.63	0.69	0.34	1.00	0.82	0.25	0.72	0.72	0.72	0.70
Ni	0.59	0.56	0.65	0.65	0.05	–0.70	–0.44	–0.23	0.74	0.79	0.87	0.51	0.69	0.65	0.86	0.68	0.72	0.79
Cu	0.61	0.53	0.83	0.10	–0.16	–0.66	0.15	–0.27	0.74	0.82	0.39	0.79	0.83	0.73	0.66	0.79	0.83	0.81
Rb	–0.46	–0.15	0.10	–0.05	–0.41	0.32	0.15	0.74	–0.33	–0.16	–0.33	–0.09	–0.38	–0.24	–0.55	–0.24	–0.21	–0.24
Sr	–0.82	–0.52	–0.69	–0.41	–0.19	0.72	0.36	0.47	–0.73	–0.76	–0.75	–0.59	–0.67	–0.84	–0.88	–0.68	–0.71	–0.80
Y	0.75	0.59	0.79	0.11	0.01	–0.73	–0.14	–0.41	0.90	0.95	0.61	0.82	–	0.82	0.80	0.99	0.99	0.91
Zr	0.73	0.35	0.54	0.23	0.08	–0.67	–0.14	–0.23	0.55	0.67	0.59	0.25	0.82	–	0.81	0.56	0.65	0.63
Nb	0.81	0.65	0.82	0.42	0.10	–0.82	–0.49	–0.51	0.86	0.93	0.80	0.72	0.80	0.81	–	0.80	0.83	0.93
Cs	–0.45	–0.18	0.02	–0.08	–0.35	0.32	0.03	0.68	–0.27	–0.16	–0.29	–0.18	–0.33	–0.24	–0.53	–0.21	–0.19	–0.26
Ba	0.20	0.19	0.41	–0.12	–0.20	–0.27	0.73	–0.04	0.28	0.35	0.00	0.36	0.38	0.37	0.09	0.35	0.39	0.40
La	0.53	0.63	0.71	0.21	0.01	–0.63	–0.20	–0.30	0.93	0.93	0.69	0.72	0.99	0.56	0.80	–	0.98	0.91
Yb	0.60	0.62	0.77	0.21	–0.01	–0.69	–0.18	–0.27	0.91	0.95	0.69	0.72	0.99	0.65	0.83	0.98	–	0.93
Hf	0.71	0.48	0.67	0.30	0.10	–0.70	–0.30	–0.31	0.71	0.76	0.67	0.52	0.77	0.79	0.88	0.71	0.76	0.78
Ta	0.48	0.62	0.64	0.62	0.10	–0.64	–0.47	–0.36	0.75	0.77	0.85	0.46	0.56	0.44	0.87	0.63	0.65	0.85
Th	0.60	0.69	0.83	0.40	0.01	–0.74	–0.23	–0.31	0.91	0.97	0.79	0.70	0.91	0.63	0.93	0.91	0.93	–
U	0.49	0.61	0.72	0.22	–0.06	–0.61	0.09	–0.31	0.88	0.88	0.62	0.70	0.90	0.56	0.73	0.91	0.91	0.91

plot shows that the Crow Creek Member is composed of components from sources ranging from mafic igneous, intermediate igneous to quartzose sedimentary compositions.

Evidence from Trace Elements

The elements Co, Ni, Cr, Sc, Zr, Hf, Nb, Ta, Th, and the REE are considered to have low mobility during sedimentary processes, and are regarded to be the most useful for provenance characterization (Taylor and McLennan 1985; Bhatia and Crook 1986). The elements Zr, Hf, La, and Th are more concentrated in felsic rocks than in basic rocks, while Cr, Ni, Co, Sc, Ta, and Nb are more concentrated in basic rocks than in felsic rocks. These elements are mainly transported in the terrigenous component of sediment and therefore reflect the composition of the source materials (McLennan et al. 1980). However, because actual concentrations can vary due to many reasons, ratios of these elements such as La/Co, Th/Co, Cr/Th, La/Sc are considered to be relatively insensitive to weathering, alteration and metamorphism and are therefore more reliable (Cullers 1995; Condie and Wronkiewicz 1990). The Cr-Th ratios are remarkably variable (GC = 8.27–10.0; IC = 7.99–83.3; and WLQ = 22.8–121) reflecting a higher input of basic material than felsic material. In contrast, the Th-Sc ratios are quite uniform ranging form 0.84 to 1.70 (except GG239.9 at 3.72) and are comparable to that of NASC (0.83). The Th-Sc and other ratios (Tables 4a–4c) suggest almost equal contributions from both basic and felsic sources. On bivariate diagrams of trace element ratios represented by Co/Th-Th/Sc, Co/Th-La/Sc, and Cr/Th-La/Sc; both felsic and basic, only felsic and only basic sources are reflected, respectively (Figs. 11a–11c). The bulk of the samples are composed of quartz, carbonates,

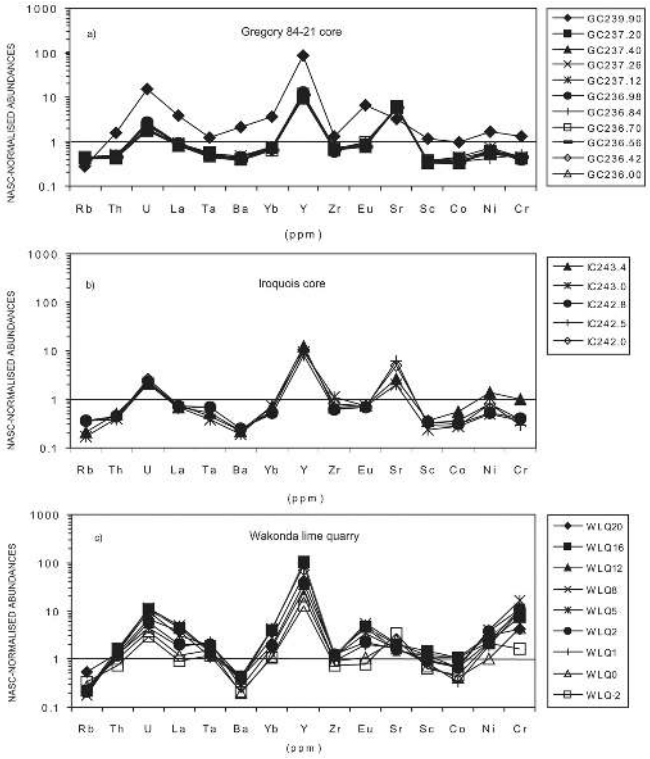

Fig. 8. North American Shale Composite (NASC)-normalized (Gromet et al. 1984) diagrams of trace elements for the Crow Creek Member samples: a) Gregory 84-21 core; b) Iroquois core; and c) Wakonda lime quarry.

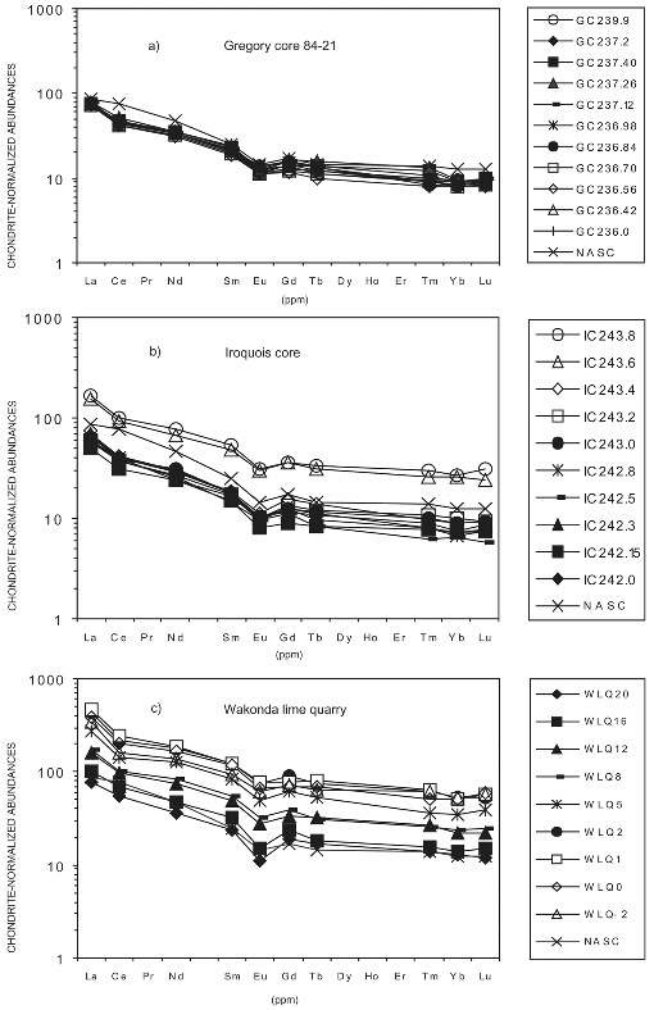

Fig. 9. Chondrite-normalized (Taylor and McLennan 1985) rare earth elements (REE) distribution patterns for the Crow Creek Member samples. North American Shale Composite (NASC) is included for comparison. All the samples have similar fractionated patterns showing small negative Eu-anomalies and flat heavy rare earth element patterns (HREE): a) Gregory 84-21 core; b) Iroquois core; and c) Wakonda lime quarry.

and minor feldspar, which do not host the trace elements used in the evaluation. However, the mixed felsic and basic provenance is reflected by the mineralogical composition of the phosphates (REE, Th), clay minerals (REE, Fig. 13), and the heavy and magnetic mineral fractions. The heavy and magnetic mineral fractions consists mainly of zircon (Th, Zr, Hf, La), sphene (Th, Hf), hematite, magnetite and other oxide and sulphide phases (Cr, Sc), which are the principal carriers of the corresponding trace elements and others (Condie and Wronkiewicz 1990).

To further evaluate the bulk source-rock composition, contents of Th, Hf, Zr, La, Co, and Sc are plotted on Th-Hf-Co, La-Cr-Zr and Th-Hf-Sc ternary diagrams (Figs. 11a–11c). The Th-Hf-Co diagram shows weak dispersion of points in the central area, but most of the points plot close to the Th-Co boundary. On the La-Cr-Zr diagram, the samples plot close to the Zr-Cr boundary away from La apex. This plot discriminates fairly well, samples of higher contents of felsic (GC and some IC samples) and basic derivatives (WLQ and some IC samples). On the Th-Hf-Sc diagram almost all the samples cluster close the Th-Sc boundary in the middle and away from the Hf apex. Chondrite-normalized REE distribution patterns for all the samples are similar to that of NASC, suggesting that the source rocks of the Crow Creek Member had a typical fractionated upper continental crust composition. Light rare earth elements (LREE), represented by La show good positive correlations with P_2O_5 (r = 0.85–0.91), suggesting that phosphate phases are the principal host of the LREE (Fig. 13a). Moderate positive correlation with Al_2O_3 (r = 0.62–0.70) indicates that LREE are controlled to a lesser extent by clay minerals (Fig. 13b). Correlation coefficients between REE and Zr are moderate, ranging from +0.50 to +0.62. P_2O_5 is represented by apatite, which occurs as pellets or concretions around bone or fish-scale fragments, and as coatings around quartz (Witzke et al. 1996). This suggests that apatite was locally derived and was liable to dissolution and later redeposited. REEs are generally considered immobile elements, which are not affected by diagenetic or metasomatic processes. In the case where they are hosted by a soluble mineral such as apatite, under certain conditions the REE will also go into solution and redistributed. In this context, LREE may have been locally

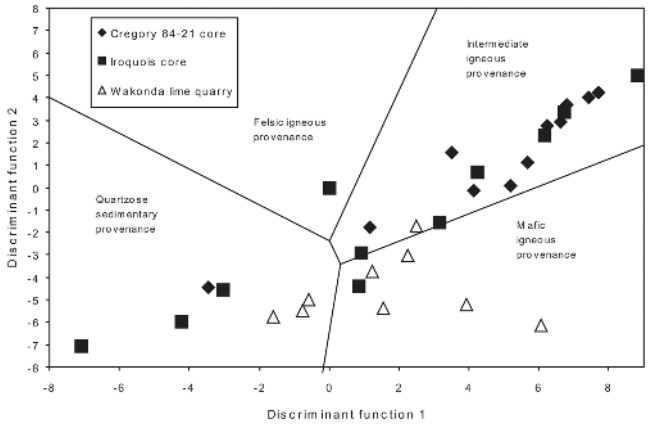

Fig. 10. Discriminant function for provenance signatures of sandstone-mudstone suites using major elements (after Roser and Korsch 1988). The plot shows mixed provenance for the Crow Creek Member samples.

redistributed by diagenetic/metasomatic processes. Europium is not fractionated during weathering or diagenesis relative to other REE (McLennan 1989). The slight negative Eu-anomalies exhibited in the REE distribution patterns of the samples may be due to minor inputs from Eu-depleted felsic igneous source rock. The Eu-anomalies (Eu/Eu* = 0.54–0.8) are similar to that of mean values of NASC (0.66; Gromet et al. 1984).

The major target rocks in the Manson impact crater region comprise, shale, sandstone, siltstone, amphibolite and biotite gneiss, granite and carbonate (Koeberl et al. 1996). This mixed composition of target rocks, coupled with the indigenous inputs, is reflected in the mixed felsic and basic bulk components in the Crow Creek Member samples we studied.

Weathering

Various indices of chemical weathering have been proposed based on different molecular proportions of immobile-element oxides (Al_2O_3, ZrO_2 and TiO_2) relative to mobile elements (Na_2O, CaO, MgO, K_2O) (Chittleborough 1991). The chemical index of alteration (CIA), chemical index of weathering (CIW) and the Al_2O_3-(CaO*+Na_2O)-K_2O (A-CN-K) ternary diagram, are widely used to constrain paleoweathering conditions of ancient fine-grained sediments (Nesbitt and Young 1982; Fedo et al. 1995; Nesbitt et al. 1997).

The CIA and CIW are calculated as (Al_2O_3/[Al_2O_3+CaO*+Na_2O+K_2O])*100 and (Al_2O_3/[Al_2O_3+CaO*+Na_2O])*100, respectively, where the oxides are expressed as molar proportions and CaO* is the concentration of CaO in silicates only. However, CaO values in our samples are high and variable, ranging from 7 to 30 wt%, mainly due to the presence of carbonates and phosphates. Fedo et al. (1995) proposed a correction, which involves CO_2 contents in rocks with CaO contributions from non-silicate minerals. In this study we did not analyze for

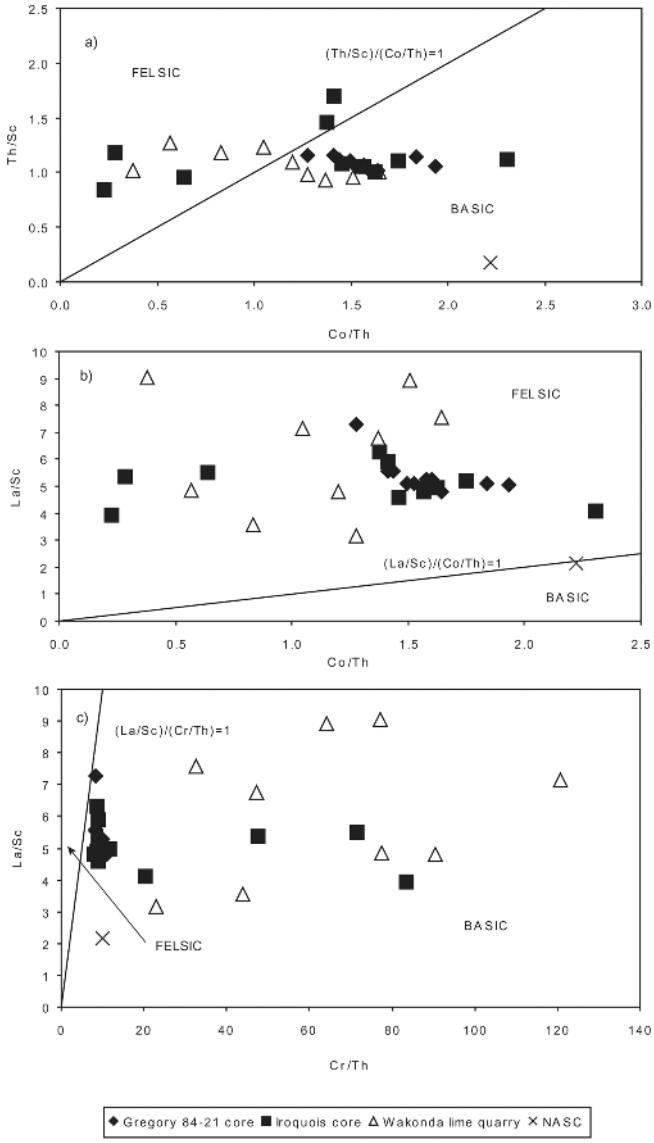

Fig. 11. Trace element ratio diagrams of: a) Co/Th-Th/Sc; b) Co/Th-La/Sc; and c) Cr/Th-La/Sc. The straight line represents 1:1 ratio, between element ratios, and discriminates samples with more felsic and basic derivates.

CO_2, thus there is no easy way to distinguish CaO contributions from carbonates and silicates (feldspars). The main silicate host of CaO, plagioclase is rare in our samples, and sphene, the only other Ca-silicate occurs as an accessory mineral, thus molar CaO* contributions from silicates in the calculation would be negligible. To this effect, CaO* is deliberately omitted in the CIA and CIW calculations and the corresponding indices adopted in this study are designated CIA' and CIW', respectively, which are close and reasonable approximations of the former (Cullers 2000). Similarly, the A-CN'-K diagram is adapted from the A-CN-K diagram (Nesbitt and Young, 1984) following the omission of CaO*. CIA values indicate the nature and degree of weathering to which the sedimentary rocks have been subjected (e.g., CIA =

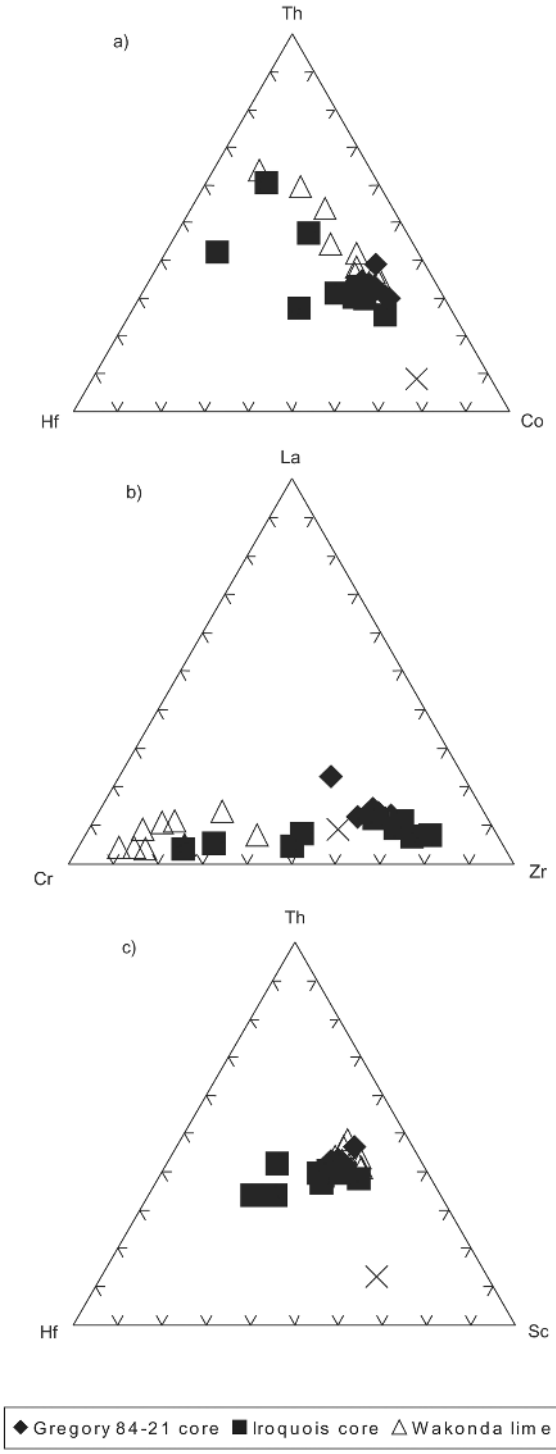

Fig. 12. Ternary diagrams of trace element contents, which reflect provenance: a) Th-Hf-Co; b) La-Cr-Zr; and c) Th-Hf-Sc. All plots indicate a mixed provenance for the Crow Creek Member samples.

50 for fresh rocks, 70–75 for shale and 100 for highly weathered rocks) (Nesbitt and Young 1982). The Crow Creek samples yield moderate to high CIA' values (72–92) and high CIW' values (85–99), with higher values represented by WLQ samples.

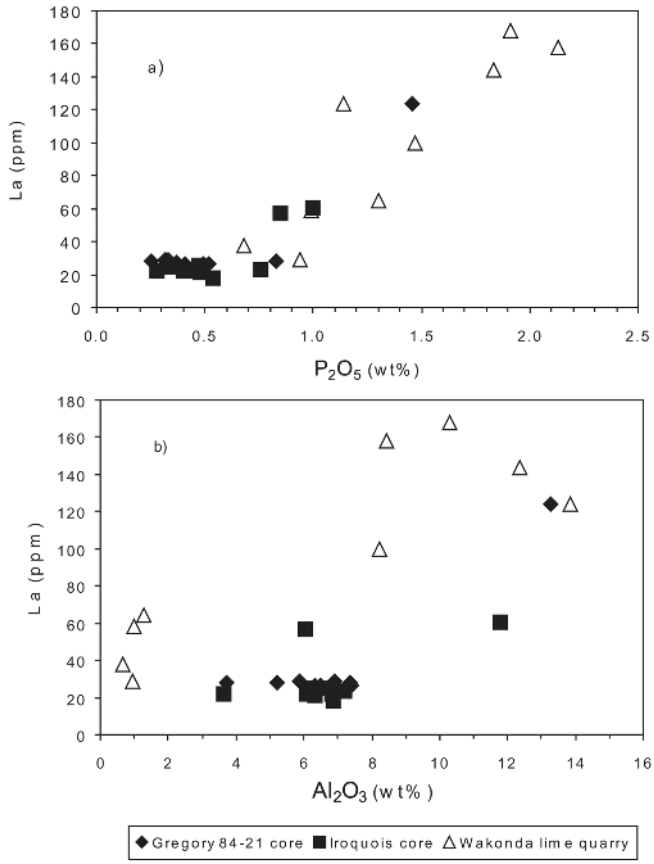

Fig. 13. Correlation of major elements with rare earth element (REE) (La): a) P_2O_5-La; and b) Al_2O_3-La. Other REE show similar trends.

On the A-CN'-K ternary diagram most of the samples plot close to the AK boundary and the A apex (Fig. 14). WLQ samples, which plot very close to the AK boundary, are characterized by high CIA' values, ranging from 88–93, (CIW' = 98–99) suggesting advanced weathering of sediment and source. The GC, IC, and NASC samples cluster in the same region close to the A apex, with CIA' values varying from 75–83 (CIW' = 85–92). The GC and IC sample points apparently follow a crude metasomatic trend towards the K apex (Fedo et al. 1995). The CIA' and CIW' indices, and A-CN'-K plot of the Crow Creek Member samples indicate that the samples and source rocks are highly weathered, especially the WLQ samples. The A-CN'-K diagram also shows that all the sample points are confined within the weathering trends of average compositions of gabbro, granodiorites, and granites (Nesbitt and Young 1984); an observation which further supports a mixed provenance.

Meteoritic Components

Siderophile elements (Cr, Co, and Ni), including the PGEs, have high abundances in meteorites, but low abundances in terrestrial crustal rocks, and are generally used to detect a meteoritic component in impactites (see review in

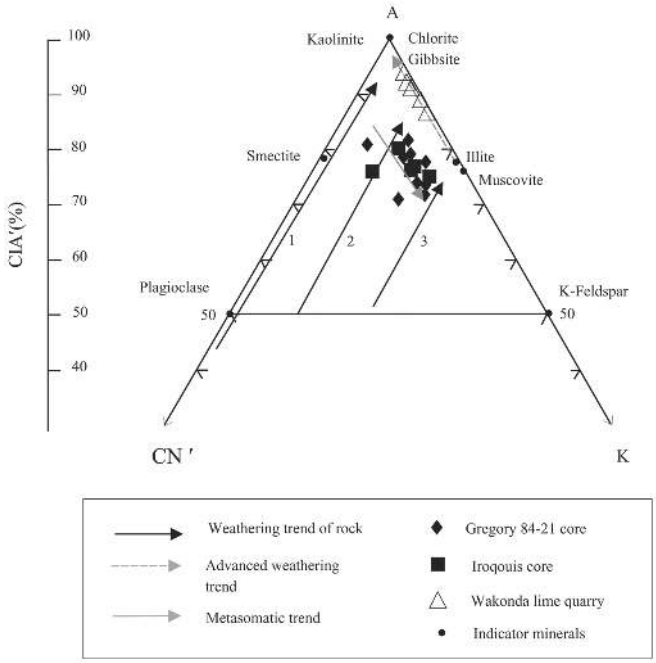

Fig. 14. Al_2O_3-(CaO*+Na_2O)-K_2O (A-CN'-K) diagram (Nesbitt and Young 1984) for the Crow Creek Member samples, where CaO* is the concentration of CaO in silicates only. The CaO* content in the Crow Creek Member samples are ignored for reasons explained in the text. CIA' = molar (Al_2O_3/(Al_2O_3+CaO*+Na_2O+K_2O)). Numbers 1-3 denote compositional trends of initial weathering profiles of average compositions of various igneous rocks types (after Nesbitt and Young 1984). 1-gabbro; 2-granodiorite; and 3-granite.

Koeberl 1998). Results of our preliminary iridium analyses in most samples fall within the range of detection limits (0.5 to 2.0 ppb) of INAA. The contents of Cr and Ni are depleted in most samples from GC and IC and enriched in all the basal-unit samples relative to those of NASC. Variable correlation coefficients between Cr, Co, Ni, and P_2O_5, Fe_2O_3, TiO_2, and Al_2O_3 suggest the distribution of these elements in different mineral phases, i.e., phosphates, Fe-Ti oxides and clay minerals. This also reflects the interplay between source rock, transportation and diagenetic/metasomatic processes. Poor correlation with MgO (r = +0.18) indicates that the metals are not associated with ferromagnesian minerals. Because contents of Cr, Co and Ni in terrestrial rocks are generally variable, and may be high due to local sources, such as sulphides and oxides of these elements (e.g., chromite [$FeCr_2O_4$], magnetite [$(Fe, Cr)_3O_4$], carrollite [$Cu(Co, Ni)_2S_4$], pentlandite [$(Fe, Ni)_9S_8$], etc), the sources of the elements are ambiguous (Koeberl 1998). Although chemical compositional differences between the basal unit and the upper marly layer are not very distinct and vary from one sample suite to the other, contents of Sc, V, Cr, and Ni are marginally higher in the basal units than in the marly layers.

The contents of Cr (54–103 ppm), Co (14–28 ppm) and Ni (28–66 ppm) determined by Pernicka et al. (1996) impact melt rocks and breccias from M1 core from the central uplift of the Manson crater are significantly lower than contents in our samples. The higher contents in Crow Creek Member samples could be due to concentration by heavy mineral sorting during transportation. A meteoritic component in the impactites at the MIS was confirmed by slightly elevated PGE abundances (Pernicka et al. 1996) and characteristic Os isotopic compositions (Koeberl and Shirey 1996), but, in general, rather low contents of meteoritic elements were observed. For our samples, the elevated Cr, Co, and Ni contents in the basal-unit samples can be taken to indicate a meteoritic component, but unfortunately the Ir contents are at or near the limit of detection. Together with the fairly low PGE abundances observed in Manson impact melt rocks and breccias, the Ir contents in the Crow Creek samples do not provide an unambiguous impact marker.

Thickness of the Ejecta Layer

There are several different empirically derived formulas that describe the thickness of ejecta blankets with distance from the crater (e.g., McGetchin et al. 1973; Melosh 1989). One of the most commonly used formulae, after McGetchin et al. (1973) gives a power law for the ejecta blanket (t) as a function of distance from the crater center:

$$t = 0.14R^{0.74}(r/R)^{-3.0}$$

where R is the radius of the transient cavity and r is the distance of ejecta from the center of the crater, and all dimensions are in meters.

As a first approximation, the thicknesses of ejecta (t) at our sample locations were calculated using the final radius, R′ (18.5 km) of the MIS. At distances (r) from the MIS to the sample locations, i.e., GC (r = 409 km), IC (r = 300 km), and WLQ (r = 219 km), thicknesses (t) calculated with the equation of McGetchin et al. (1973) are: GC = 1.9 cm; IC = 4.7 cm, and WLQ = 12.2 cm. Thicknesses of basal units of the Crow Creek Member at GC, IC, and WLQ sample locations are 3, 25, and 25 cm, respectively. Using a transient cavity radius of about 2/3 of the final crater radius (Melosh 1989), i.e., about 12 km, we arrive at thicknesses of 0.37, 0.94, and 2.4 cm for GC, IC, and WLQ, respectively.

The results show that, as expected, the thickness of ejecta in the Crow Creek Member is inversely proportional to the distance from the MIS. The calculated thickness of ejecta at the site of Gregory core 84-21 (farthest from the MIS) is less than that at Wakonda lime quarry (nearest to the MIS). This is generally consistent with the observed regional variation in thickness of the basal unit of the Crow Creek Member, which is thicker in the eastern location (WLQ sample location) and thinner in the western setting (GC sample location). However, the calculated thicknesses of Manson ejecta at our sample locations are thinner than the observed basal unit thicknesses. The most likely reason for this is that not all of the basal unit comprises actual impact ejecta, and because paleotopography

and post-depositional changes can easily alter local thicknesses.

CONCLUSIONS

We conducted whole-rock chemical analyses and shock petrographic studies of the basal and marly units of the Crow Creek Member from South Dakota. The basal unit of the Crow Creek Member contains ejecta material from the 74-Ma Manson impact structure. The following conclusions can be drawn from the present study:

1. The felsic contents in the samples vary from one sample suite to the other with higher contents generally occurring in the basal-unit samples, ranging from 3–34 wt%, but there is no systematic trend from the base to the top in felsic contents. The bulk of the felsic residues range in grain size from 125 to 250 μm.
2. Shocked minerals (total of 14 grains) mainly quartz are very rare and were only found in the basal unit of the Crow Creek Member i.e., GC239.9, IC243.6, IC243.8 and WLQ8-12. The shocked minerals display mosaicsm and contained up to three sets of fresh PDFs, with crystallographic orientations: $\{10\bar{1}3\}$, $\{10\bar{1}2\}$, $\{10\bar{1}1\}$, $\{01\bar{1}1\}$, and $\{11\bar{2}1\}$ (ω, π, r, z, and s, respectively) indicating shock pressures ≥15 GPa.
3. Although the contents of Ir and other siderophile elements are higher than those measured in drill core samples from the MIS in other studies, where meteoritic components have been confirmed, a meteoritic component in Crow Creek Member samples cannot be unambiguously corroborated due to measurement (Ir) and source compositional (Cr, Co and Ni) uncertainties. In general, chemical compositional differences between the basal unit and the upper marly layer are not very distinct and vary from one sample suite to the other. However, the elements Sc, V. Cr, and Ni are marginally higher in the basal units than in the marly layers.
4. Total REE contents in the basal-unit samples are significantly higher that in the corresponding overlying marly layers. Chondrite-normalized REE distribution patterns are similar to that of NASC. Slight negative Eu-anomalies suggest inputs from Eu-depleted felsic igneous source rocks.
5. When compared to NASC, the samples are high in contents of CaO, MnO, P_2O_5, Sr, U, and Y. The high contents in these elements are due to the presence of significant amounts of carbonates (calcite and dolomite) and phosphates (apatite). P_2O_5 has good positive linear correlation coefficients with Y and REE, indicating that the distributions of these elements are controlled by phosphate minerals mainly apatite.
6. In spite of some uncertainties, i.e., potential recycling of previously weathered detritus; metasomatic effects; and the assumption made concerning CaO* contents; the CIA' and CIW' indices, and A-CN'-K plot, indicate that the Crow Creek Member and its source rocks have both been subjected to high degrees of alteration and weathering, respectively. The weathering trends of the samples, especially GC and IC, are similar to those of average compositions of gabbro, granodiorite and granite, consistent with lithologies found in the environs of the MIS.
7. Results of major and trace element abundances and elemental ratios critical to provenance studies (e.g., La/Co, Th/Co, Cr/Th, La/Sc, Eu/Eu*), coupled with accessory mineral compositions, suggest that the source rocks of the Crow Creek Member are of mixed provenance, ranging from quartzose, intermediate and mafic compositions derived in part from the MIS region.
8. Somewhat elevated Cr, Co, and Ni abundances in the basal-unit samples compared to other samples might indicate the presence of a meteoritic component, although low Ir value (at or near the limit of detection) do not allow unambiguous confirmation of this suggestion.
9. The thicknesses of Manson ejecta in South Dakota have been calculated to range from 1.9 to 12.2 cm, using the observed crater diameter, and 0.37 to 2.4 cm, using an estimated transient cavity radius of 12 km, for the sample locations that are at distances ranging from 219 to 409 km from the crater center. The observed thicknesses of the Crow Creek basal unit are thicker than the calculated values, probably because not all of the basal unit comprises impact ejecta, and due to paleotopographic variations.

Acknowledgments–A Ph.D. stipend from the Austrian Academic Exchange Service (ÖAD) to C. Katongo is gratefully acknowledged. Field and Laboratory work were supported by the Austrian FWF project Y58-GEO to C. Koeberl. We thank Kelli McCormick and her colleagues of the South Dakota Geological Survey, Vermillion, South Dakota, for help with core access, and for permission to take the samples. We thank W. U. Reimold (University of the Witwatersrand, Johannesburg) for XRF analyses and U. Klötzli (University of Vienna) for use of the Franz isodynamic magnetic separator. Constructive comments from the associate editor R. A. F Grieve and two anonymous reviewers are greatly appreciated.

Editorial Handling—Dr. Richard Grieve

REFERENCES

Alvarez L. W, Alvarez W., Asaro F., Michel H. V. 1980. Extraterrestrial cause for the Cretaceous-Tertiary extinction. *Science* 208:1095–1108.

Anderson R. R. 1987. Precambrian Sioux Quartzite at Gitchie Manitou State Preserve, Iowa. In *Centennial Field Guide 3,* edited by Biggs D. L. Washington D.C.: Geological Society of America. pp. 77–80.

Bhatia M. R. and Crook K. A. W. 1986. Trace element characteristics

of greywackes and tectonic discrimination of sedimentary basins. *Contributions to Mineralogy and Petrology* 92:181–193.

Bohor B. F., Foord E. E., Modreski P. J., and Triplehorn D. M. 1984. Mineralogical evidence from am impact event at the Cretaceous-Tertiary boundary. *Science* 224:867–869.

Bretz R. F. 1979. Stratigraphy, mineralogy, paleontology and paleoecology of the Crow Creek Member, Pierre Shale (late Cretaceous), south central South Dakota. M.Sc. thesis, Fort Hays State University, Hays, Kansas, USA.

Chittleborough D. J. 1991. Indices of weathering in soils and palaeosols formed on silicate rocks. *Australian Journal of Earth Sciences* 38:115–120.

Condie K. C. and Wronkiewicz D. J. 1990. The Cr/Th ratio in Precambrian pelites from the Kaapvaal Craton as an index of craton evolution. *Earth and Planetary Science Letters* 97:256–267.

Cox R., Low D. R., and Culler R. L. 1995. The influence of sediment recycling and basement composition on evolution of mud-rock chemistry in the southwestern United States. *Geochimica et Cosmochimica Acta* 59:2919–2940.

Crandell D. R. 1952. Origin of the Crow Creek Member of Pierre Shale in central Dakota. *American Association of Petroleum Geologists Bulletin* 36:1754–1765.

Cullers R. L. 1995. The controls of the major and trace-element evolution of shales, siltstones and sandstones of Ordovician to Tertiary age in the Wet Mountains region, Colorado USA. *Chemical Geology* 123:107–131.

Cullers R. L. 2000. The geochemistry of shales, siltstones and sandstones of the Pennsylvanian-Permian age, Colorado, USA: implications for provenance and metamorphic studies. *Lithos* 51: 181–203.

Engelhardt W. V. and Bertsch W. 1969. Shock induced planar deformation structures in quartz from the Ries crater, Germany. *Contributions to Mineralogy and Petrology* 20:123–234.

Fedo C. M., Nesbitt H. W., and Young G. M. 1995. Unraveling the effects of potassium metasomatism in sedimentary rocks and paleosols, with implications for paleo-weathering conditions and provenance. *Geology* 23:921–924.

French B. M. 1998. Traces of catastrophe: A handbook of shock Metamorphic effects in terrestrial Meteorite Impact Structures. LPI Contributions No. 954. Houston: Lunar and Planetary Institute. 120 p.

Grieve R. A. F. and Therriault A. M. 1995. Planar deformation features in quartz: Target effect (abstract). 26th Lunar and Planetary Science Conference. pp. 515–516.

Grieve R. A. F., Langenhorst F., and Stöffler D. 1996. Shock metamorphism of quartz in nature and in experiment: II Significance in geosciences. *Meteoritics & Planetary Science* 25: 1530–1534.

Gromet L. P., Dymek R. F., Haskin L. A., and Korotev R. L. 1984. The North American Shale Composite: Its implications, major and trace elements characteristics. *Geochimica et Cosmochimica Acta* 48:2469–2482.

Izett G. A., Cobban W. A., Obradovich G. B., and Kunk M. J. 1993. The Manson impact structure: $^{40}Ar/^{39}Ar$ age its distal impact ejecta in the Pierre Shale in southeastern South Dakota. *Science* 262:729–732.

Izett G. A., Cobban W. A., and Obradovich G. B. 1998. $^{40}Ar/^{39}Ar$ age of the Manson impact structure, Iowa and correlative impact ejecta in the Crow Creek Member of the Pierre Shale (Upper Cretaceous) South Dakota and Nebraska. *Geological Society of America Bulletin* 110:361–376.

Koeberl C. 1993. Instrumental neutron activation analysis of geological and cosmochemical samples: A fast and proven method for small samples analysis. *Journal of Radioanalytical and Nuclear Chemistry* 168:47–60.

Koeberl C. 1998. Identification of meteoritic components in impactites. In *Meteoritics: Flux with time and impact effects,* edited by Grady M. M., Hutchison R., McCall G. J. H., and Rothery D. A. Geological Society of London Special Publication 140. pp.133–153.

Koeberl C. 2001. The sedimentary record of impact events. In *Accretion of extraterrestrial matter throughout Earth's history,* edited by Peucker-Ehrenbrink B. and Schmitz B. New York: Kluwer Academic/Plenum Publishers. pp. 333–378.

Koeberl C. and Anderson R. R. 1996. Manson and company: Impact structures in the United States. In *The Manson impact structure, Iowa: Anatomy of an impact crater,* edited by Koeberl C. and Anderson R. R., Geological Society of America Paper 302. pp. 1–29.

Koeberl C. and Shirey S. B. 1993. Detection of a meteoritic component in Ivory Cost tektites using rhenium-osmium systematics. *Science* 261:595–598.

Koeberl C. and Shirey S. B. 1996. Re-Os isotope study of rocks from the Manson impact structure. In *The Manson impact structure, Iowa: Anatomy of an impact crater,* edited by Koeberl C. and Anderson R. R. Geological Society of America Special Paper 302. pp. 331–339.

Koeberl C. and Shirey S. B. 1997. Re-Os systematics as a diagnostic tool for the study of impact craters and distal ejecta. *Palaeogeography, Palaeoclimatology, Palaeoecology* 132:25–46.

Koeberl C. and Sigurdsson H. 1992. Geochemistry of impact glasses from the K/T boundary in Haiti: Relation to smectites, and a new type of glass. *Geochimica et Cosmochimica Acta* 56:2113–2129.

Koeberl C., Reimold W. U., Kracher A., Träxler B., Vormaier A., and Körner W. 1996. Mineralogical, petrological, and geochemical studies of drill core samples from the Manson impact structure, Iowa. In *The Manson impact structure, Iowa: Anatomy of an impact crater,* edited by Koeberl C. and Anderson R. R., Geological Society of America Special Paper 302. pp. 145–218.

McGetchin T. R., Settle M., and Head J. W. 1973. Radial thickness variation in impact crater ejecta: Implications for lunar basin deposits. *Earth and Planetary Science Lettters* 20:226–236.

McLennan S. M. 1989. Rare earth elements in sedimentary rocks: influence of provenance and sedimentary processes. In: *Geochemistry and mineralogy of rare Earth elements,* edited by Lipin B. R., and McKay G. A. *Reviews in Mineralogy* 21:169–200.

McLennan S. M., Nance W. B., and Taylor S. R. 1980. Rare earth element-thorium correlations in sedimentary rocks and the composition of the continental crust. *Geochimica et Cosmochimica Acta* 44:1833–1839.

McLennan S. M. and Taylor S. R. 1982. Geochemical constraints on the growth of continental crust. *Journal of Geology* 90:347–361.

McLennan S. M., Hemming S., McDaniel D. K., and Hanson G. N. 1993. Geochemical approaches to sedimentation, provenance and tectonics. In *Processes controlling the composition of clastic sediments,* edited by Johnsson M. J. and Basu A. Geological Society of America Special Paper 284. pp. 21–40.

Melosh H. J. 1989. *Impact cratering.* New York: Oxford University Press. 245 p.

Montanari A. and Koeberl C. 2000. *Impact stratigraphy: The Italian record. Lecture notes in earth sciences 93.* Heidelberg: Springer-Verlag. 364 p.

Nesbitt H. W. and Young G. M. 1982. Early Proterozoic climates and plate motions inferred from major element chemistry of lutites. *Nature* 199:715–717.

Nesbitt H. W. and Young G. M. 1984. Prediction of some weathering trends of plutonic and volcanic rocks based on thermodynamics and kinetic considerations. *Geochimica et Cosmochimica Acta* 48:1523–1534.

Nesbitt H. W., Fedo C. M., and Young G. M. 1997. Quartz and

feldspar stability, steady and no-steady state weathering and petrogenesis of siliciclastic sands and muds. *Journal of Geology* 105:173–191.

Pernicka E., Kaether D., and Koeberl C. 1996. Siderophile element concentrations in drill core samples from the Manson crater. In *The Manson impact structure, Iowa: Anatomy of an impact crater,* edited by Koeberl C. and Anderson R. R., Geological Society of America Special Paper 302. pp. 325–330.

Reimold W. U., Koeberl C., and Bishop J. 1994. Roter Kamm impact crater, Namibia: Geochemistry of basement rocks and breccias. *Geochimica et Cosmochimica Acta* 58:2689–2710.

Roser B. P. and Korsch R. J. 1988. Provenance signatures of sandstone-mudstone suites determined using discriminant function analysis of major elemental data. *Chemical Geology* 67: 119–139.

Schultz L. G. 1965. *Mineralogy and stratigraphy of the lower part of the Pierre Shale, South Dakota and Nebraska.* U.S. Geological Survey Professional Paper 392-B. 19 p.

Steiner M. B. and Shoemaker E. M. 1996. A hypothesized Manson impact tsunami: Paleomagnetic and stratigraphic evidence in the Crow Creek Member, Pierre Shale. In *The Manson impact structure, Iowa: Anatomy of an impact crater,* edited by Koeberl C. and Anderson R. R. Geological Society of America Special Paper 302. pp. 419–431.

Stöffler D. and Langenhorst F. 1994. Shock metamorphism of quartz in nature and experiment: I. Basic observations and theory. *Meteoritics* 29:155–181.

Taylor S. R. and McLennan S. M. 1985. *The continental crust: Its composition and evolution. An examination of the geochemical record preserved in sedimentary rocks.* Oxford: Blackwell Scientific Publications. 312 p.

Witzke B. J., Ludvigson G. A., Poppe J. A., and Ravn R. L. 1983. Cretaceous paleogeography along the eastern margin of the western Interior Seaway, Iowa, southern Minnesota, and eastern Nebraska and South Dakota. In *Rocky Mountain paleogeography symposium 2, Rocky Mountain section,* edited by Reynolds M. W. and Dolly E.D. Society of Economic Paleontologists and Mineralogists. pp. 225–253.

Witzke B. J, Hammond R. H., and Anderson R. R. 1996. Deposition of the Crow Creek Member, Campanian, South Dakota and Nebraska. In *The Manson impact structure, Iowa: Anatomy of an impact crater,* edited by Koeberl C. and Anderson R. R. Geological Society of America Special Paper 302. pp. 433–456.